

Analysis of Pion Photoproduction Data

R. A. Arndt^{*}, W. J. Briscoe[†], I. I. Strakovsky[‡], R. L. Workman[§]

*Center for Nuclear Studies, Department of Physics,
The George Washington University, Washington, D.C. 20052*

(October 24, 2018)

Abstract

A partial-wave analysis of single-pion photoproduction data has been completed. This study extends from threshold to 2 GeV in the laboratory photon energy, focusing mainly on the influence of new measurements and model-dependence in the choice of parameterization employed above the two-pion threshold. Results are used to evaluate sum rules and estimate resonance photo-decay amplitudes. These are compared to values obtained in the MAID analysis.

PACS numbers: 11.80.Et, 14.20.Gk, 25.20.Lj

Typeset using REVTeX

^{*}arndt@reo.ntelos.net

[†]briscoe@gwu.edu

[‡]igor@gwu.edu

[§]rworkman@gwu.edu

I. INTRODUCTION

Meson-nucleon scattering, meson photoproduction, and meson electroproduction have been extensively studied within a comprehensive program exploring the spectroscopy of N^* and Δ^* resonances. An objective of this program is the determination of all relevant characteristics of these resonances, *i.e.* pole positions, widths, principal decay channels, and branching ratios. In order to compare directly with QCD-inspired models, there has also been a considerable effort to find “hidden” or “missing” resonances, predicted by quark models (see, for example, the states predicted by Capstick and Roberts [1]) but not yet confirmed.

Here we will give detailed results from an ongoing analysis of pion photoproduction data. This work complements our studies of pion-nucleon elastic scattering [2], both reactions having the same resonance content, and provides the real-photon limit for our pion-electroproduction fits [3]. Resonance characteristics are determined through a two-step procedure. The full database is initially fitted to determine the underlying multipole contributions. Those multipoles having resonant contributions are then fitted to a form containing both resonance and background terms.

The availability of multipole amplitudes greatly simplifies certain numerical aspects of coupled-channel analysis. The number of fitted multipole amplitudes, associated with a dataset, may be smaller (than the count of individual data) by one or two orders of magnitude, and can account for issues associated with statistical/systematic errors, data rejection, and incomplete sets of observables. In general, our partial-wave analyses (PWA) have been as model-independent as possible, so as to avoid bias when used in resonance extraction or coupled-channel analysis. However, in the absence of complete experimental information, all multipole analyses above the two-pion production threshold are model-dependent to some degree. This issue will be discussed in Section III.

The amplitudes from these analyses can be utilized in evaluating contributions to the Gerasimov-Drell-Hearn (GDH) sum rule [4] and sum rules related to the nucleon polarizability. We display our results for these and compare with recent Mainz experimental data and predictions.

In the next section, we summarize changes in the database since our last published analysis [5]. Results of our multipole analyses, as well as the photo-decay amplitudes for resonances within our energy region, are given in Section III. In Section IV, we summarize our findings and consider what improvements can be expected in the future.

II. DATABASE

Our three previous pion photoproduction analyses [5–7] extended to 1.0, 1.8, and 2.0 GeV, respectively. The present database [8] is considerably larger, due mainly to the addition of new data at low to intermediate (below 800 MeV) energies.

In 1994, bremsstrahlung data comprised over 85% of the existing measurements. These data often suffered from significant uncertainties in normalization that were not completely understood or not quoted. The available tagged-photon data were generally measured in low-statistics experiments, and hence were presented with large energy and angular binning. Much of the remaining dataset was comprised of excitation cross sections with no extensive

angular range. Inconsistencies were obvious almost everywhere that comparisons could be made.

The full database has increased by 30% since the publication of Ref. [5], and is about 40% larger than the set available for the analysis of Ref. [7]. The majority of these new data have come from tagged-photon facilities at MAMI (Mainz), GRAAL (Grenoble), and LEGS (Brookhaven.) [The total database has doubled over the last two decades (see Table I.)] The distribution of recent (post-1995) $\pi^0 p$ and $\pi^+ n$ data is given in Fig. 1 (there are no new $\pi^- p$ and $\pi^0 n$ data.)

As the full database contains conflicting results, some of these have been excluded from our fits. We have, however, retained all available data sets (and labeled these excluded data as “flagged”) so that comparisons can be made through our on-line facility [8]. Data taken before 1960 were not analyzed, nor were those single-angle and single-energy points measured prior to 1970. Some individual data points were also removed from the analysis in order to resolve conflicts or upon authors’ requests (since our previous analysis [5], we have flagged 950 $\pi^0 p$, 1060 $\pi^+ n$, and 150 $\pi^- p$ bremsstrahlung data taken prior to 1983.) Some of the data, listed as new, were available in unpublished form at the time of our previous analysis [5]. A complete description of the database and those data not included in our fits is available from the authors.

Since 1995, 87% (21%) of all new $\pi^0 p$ ($\pi^+ n$) data have been produced at Mainz using the MAMI facility [9–19]. These measurements of total and differential cross sections, Σ beam asymmetry, and the GDH-related quantity ($\sigma_{1/2} - \sigma_{3/2}$) have increased the database by a factor of about two over the energy range from the threshold to 800 MeV. The angular range of cross sections extends from 10° to 170° , and thus increases the sensitivity to contributions from higher partial waves.

Results from other laboratories include low-energy unpolarized $\pi^0 p$ total (47 data) and differential (198 data) cross sections measured at SAL [20,21], and $\pi^+ n$ threshold data (45 points), covering a range of 2 MeV in E_γ , produced by the TRIUMF–SAL Collaboration [22]. At energies spanning the Δ resonance, Σ (169 data) and differential cross section (157 data) for both $\pi^0 p$ and $\pi^+ n$ channels have been measured by the LEGS group at BNL [23].

In the medium-energy range, $\pi^+ n$ Σ beam-asymmetry data between 600 and 1500 MeV (329 data) have been measured at GRAAL [24,25] and $\pi^0 p$ Σ data between 500 and 1100 MeV (158 data) have been measured at the 4.5 GeV Yerevan Synchrotron [26]. Target asymmetry T measurements between 220 and 800 MeV for both $\pi^0 p$ (52 data) and $\pi^+ n$ (210 data) have come from ELSA at Bonn [27,28]. Excitation $\pi^+ n$ differential cross sections for backward scattering between 290 and 2110 MeV, also from the Bonn facility, have been replaced by finalized data [29], with final versions of other $\pi^+ n$ and $\pi^0 p$ differential cross sections expected [30–33].

Further experimental efforts will provide data in the intermediate energy region. Above 400 MeV, a large amount of new data is expected from CLAS at Hall B of Jefferson Lab [34]. Differential cross sections associated with the Mainz GDH experiment [35] (related to the double-polarization quantity E [36]) should also have an impact on the analysis when combined with 4° to 177° cross section (200 to 790 MeV) and 10° to 160° Σ beam asymmetry (250 to 440 MeV) measurements at MAMI [37]. Beam asymmetry data for π^0 photoproduction below 1100 MeV will also be available from GRAAL [38]. Of particular interest are the polarized π^0 photoproduction experiments (including the polarization transfers C_x'

and $C_{z'}$ from circularly polarized photons to recoil protons) above 800 MeV carried out in Hall A of JLab [39]. From Brookhaven, we expect final LEGS Σ beam asymmetries around the Δ resonance [40] and new radiative capture cross sections which have been taken at BNL-AGS using the Crystal Ball Spectrometer (E913/914) at p_π from 400 to 750 MeV/c ($E_\gamma = 430 - 780$ MeV) [41].

III. MULTIPOLE AND PHOTO-DECAY AMPLITUDES

A. Analysis

Fits to the expanded database were first attempted within the formalism we have used and described previously [6,7,5]. Multipoles were parameterized using the form

$$M = (Born + A)(1 + iT_{\pi N}) + BT_{\pi N} \quad (1)$$

with $T_{\pi N}$ being the associated elastic pion-nucleon T -matrix, and the terms A and B being purely phenomenological polynomials with the correct threshold properties. As in our most recent analysis [5], some multipoles were allowed an additional overall phase $e^{i\Phi}$, where the angle Φ was proportional to $(\text{Im}T_{\pi N} - T_{\pi N}^2)$. This form satisfied Watson's theorem for elastic πN amplitudes [42] while exploiting the undetermined phase for πN inelastic amplitudes. For $T_{\pi N}$, we utilized our most recent fit (SM02) to elastic scattering data [43].

New and precise Σ measurements proved difficult to describe, using this choice of phenomenology. Searching for a more successful form, we found an improved description was possible if the dependence on $(\text{Im}T_{\pi N} - T_{\pi N}^2)$ was additive rather than multiplicative. As a result, we re-fitted the full database, removing the overall phase and instead added a term of the form

$$(C + iD)(\text{Im}T_{\pi N} - T_{\pi N}^2) \quad (2)$$

with C and D again being energy-dependent polynomials.

The resulting energy-dependent solution (SM02) had a χ^2 of 35296 for 17571 ($\pi^0 p$, $\pi^+ n$, $\pi^- p$, and $\pi^0 n$) data to 2 GeV. The overall χ^2/data was significantly lower than that found in our previously published result ($\chi^2/\text{data} = 2.4$) [5]. This change is partly a reflection of the the database changes discussed in Section II. Our present and previous energy-dependent solutions are compared in Table I. As in previous analyses, we used the systematic uncertainty as an overall normalization factor for angular distributions¹. This renormalization freedom provided a significant improvement for our best fit results as shown in Table II.

In order to see if the inclusion of the full existing database had resulted in a bias towards older and possibly outdated measurements, we compared the fit quality versus measurement date. Generally, we found no problem of bias, as illustrated in Table III, where we have displayed our fit quality over the region covering the N(1535) resonance. Except for

¹For total cross sections and excitation data, we combined statistical and systematic uncertainties in quadrature.

the above mentioned Σ measurements, over this energy region, our overall fit to the most recent measurements (1985–Present) is characterized by a χ^2/data of about 1.3. For all data to 2 GeV, the data restriction yields a χ^2/data near 1.5. Unfortunately, the modern measurements do not completely overlap older data. Much of the older data is required in an analysis extending over the full resonance region.

The very low energy region is complicated by different thresholds for $\pi^0 p$ and $\pi^+ n$ final states. While we have obtained a reasonable fit to the available $\pi^0 p$ differential and total cross sections (we fit rather well the new threshold TRIUMF–SAL $\pi^+ n$ cross sections [22], and Mainz $\pi^0 p$ Σ at 160 MeV [19]), the multipole amplitudes have no cusp built into the $\pi^+ n$ threshold region.

Both energy-dependent and single-energy solutions (SES) were obtained from fits to the combined $\pi^0 p$, $\pi^+ n$, $\pi^- p$, and $\pi^0 n$ databases to 2 GeV. In Table IV, we compare the energy-dependent and single-energy results over the energy bins used in these single-energy analyses. Also listed are the number of parameters varied in each single-energy solution. A total of 148 parameters were varied in the energy-dependent analysis SM02. The extended database allowed an increase in the number of SES versus our previous result [5] over the same energy range to 2 GeV.

Fig. 2 is a plot of the energy dependent fits SM02 and SM95 over the full energy region. The SES are also shown with uncertainties coming from the error matrix. In the SES fits, initial values for the partial-wave amplitudes and their (fixed) energy derivatives were obtained from the energy-dependent solution. A comparison of global and single-energy solutions then serves as a check for structures that could have been “smoothed over” in the energy-dependent analysis. Partial waves with $J < 4$ are displayed, whereas the analysis fitted waves up to $J = 5$. Significant deviations from SM95 are visible in multipoles connected to the πN S- and P-waves, as well as D_{35} , F_{35} , and D_{13} (for the neutron.)

As mentioned above, the parametrization used in our previous analysis SM95 [5] did not allow a good fit to recent Yerevan $\pi^0 p$ [26] and GRAAL $\pi^+ n$ [24,25] Σ data (the critical range extends from 700 to 800 MeV.) For comparison purposes, in Table V, we compare SM95, SM02, and SX99. The test fit SX99 retains the form used in previous fits (as in SM95) and is applied to the present full database. One can see that recent Mainz $\pi^+ n$ ($\sigma_{1/2} - \sigma_{3/2}$) [15] data are also problematic for the SX99 fit, with the most difficult region again covering the 700 to 800 MeV range. In Fig. 3, we display the energy dependence of a differential cross section measurement [45], at a fixed angle, displaying rapid variation over the region in question. These Mainz data from 560 to 780 MeV are reasonably well reproduced ($\chi^2 = 106/76$), though not included in our analysis.

B. Comparing SAID to MAID

While the SAID and MAID analyses are qualitatively similar from threshold to 1 GeV, some significant differences exist and these have been mentioned in a recent multi-analysis study which fitted to a benchmark dataset [46]. While some multipoles show significant differences, the photo-decay amplitudes from MAID and SM95 are quite similar, with larger differences between the MAID and SM02 solutions. The data fit quality shows greater variability and a few cases are given below.

The measurement of Σ for $\pi^0 p$ at threshold (160 MeV) has been discussed in [47,48] and is particularly sensitive (Fig. 4.) The plotted curves differ mainly in the P-wave multipoles. Our SES at 162 MeV, which covers 158 – 165 MeV (see Table IV,) fits the new Mainz data [19] rather well, while the energy-dependent MAID2000 and SM02 solutions are less successful.

At higher energies, close to the upper limit of MAID, new $\pi^+ n$ Σ measurements, shown in Fig. 5, are clearly problematic. This has been used to suggest a change in the N(1650) photo-decay amplitude [24].

For the forward peaking in $\pi^+ n$ unpolarized differential cross sections, displayed in Fig. 6, the disagreement between SAID and MAID results reaches as much as 30%. In the SAID fits, some of these problems are resolved once systematic uncertainties are taken in account.

The double-polarization quantity $\vec{\gamma} \vec{p} \rightarrow \pi^0 p$, measured in the A2 Collaboration GDH experiment [15] and displayed in Fig. 7, is well described by both MAID2001 and SAID solution SM02. At higher energies, deviations become more apparent (as was also shown in Fig. 3.) CLAS at JLab [56], ELSA at Bonn [57], SPring-8 at Hyogo [58], and LEGS at Brookhaven [59] have further programs underway to study this process.

In Fig. 8, we compare our results with the MAID analysis [44]² where more substantial differences are seen for the $S_{11}pE$, $P_{13}pE$, $P_{31}pM$, and $D_{13}pE$ multipoles.

We have fitted our multipoles using a simple Breit-Wigner plus background function, as described in Ref. [6]. We have employed both single-energy and energy-dependent solutions over a variety of energy ranges in order to estimate uncertainties. A listing of our resonance couplings is given in Table VI. Here, values for the resonance mass (W_R), full width (Γ), and the decay width to πN final states (Γ_π/Γ) were taken from our elastic πN analysis [43] and were not varied in the fits and error estimates.

We find that the $S_{11}pE$ ($E_{0+}^{1/2}$) multipole is very sensitive to both the database and parametrization in the range associated with the N(1535). The range of variation, particularly large for the real part of $S_{11}pE$, is displayed in Fig. 9. This sensitivity is not surprising, as the quantity $(\text{Im}T_{\pi N} - T_{\pi N}^2)$ has a very sharp structure at the ηN threshold. This variability in the multipole amplitude is reflected in the N(1535) resonance coupling, which we feel is presently too uncertain to quote.

Other couplings significantly altered using the revised parameterization scheme include the $P_{11}(1710)$, which is still essentially undetermined, $P_{13}(1720)$, $S_{31}(1620)$, and $F_{35}(1905)$. The $F_{37}(1950)$ has an easily identifiable magnetic but, essentially no electric multipole. Multipoles associated with the $D_{35}(1930)$ show very little resonance signature.

We were particularly surprised to see a large change in the $\Delta(1232)$ photo-decay amplitudes. Comparison with our SM95 fit shows a significant decrease in cross section at the resonance position. This shift has resulted due to the inclusion of recent Mainz $\pi^0 p$ measurements [11], which are systematically lower (particularly at backward angles) than an older set of Bonn measurements. More recent Mainz fits for MAID2001 [61] give -133 ± 4 and -252 ± 6 (in $10^{-3} \text{GeV}^{-1/2}$ units) for $A_{1/2}$ and $A_{3/2}$, respectively. These results have also shifted lower and are consistent with our determination.

²This MAID solution is valid to $W = 1800$ MeV ($E_\gamma = 1250$ MeV) [60].

C. Sum Rules

The amplitudes obtained in our analyses can be used to evaluate the single-pion production component of several sum rules. The GDH integral [4] relates the anomalous magnetic moment κ , the charge e , and nucleon mass M to the difference in the total photoabsorption cross sections for circularly polarized photons on longitudinally polarized nucleons

$$I_{GDH} = \int_{\nu_0}^{\infty} \frac{\sigma_{1/2} - \sigma_{3/2}}{\nu} d\nu = -\frac{\pi e^2}{2M^2} \kappa^2, \quad (3)$$

where $\sigma_{1/2}$ and $\sigma_{3/2}$ are the photoabsorption cross sections for the helicity states 1/2 and 3/2, respectively, with ν being the photon energy. For the proton (neutron) target, Eq. (3) predicts -205 (-233) μb . The running GDH integrals for the proton and neutron are shown in Fig. 10, where a comparison with MAID is also given.

The Baldin sum rule [67] relates the sum of electric and magnetic polarizabilities of the nucleon to the total photo-absorption cross section σ_{tot}

$$I_{Baldin} = \frac{1}{2\pi^2} \int_{\nu_0}^{\infty} \frac{\sigma_{tot}}{\nu^2} d\nu = \frac{1}{2\pi^2} \int_{\nu_0}^{\infty} \frac{\sigma_{1/2} + \sigma_{3/2}}{2\nu^2} d\nu. \quad (4)$$

For the proton (neutron) target, the recent dispersion calculations by Levchuk and L'vov give $(14.0 \pm 0.3)10^{-4} fm^3$ [$(15.2 \pm 0.5)10^{-4} fm^3$] [68]. For the proton, an independent Mainz determination gives $(13.8 \pm 0.4)10^{-4} fm^3$ [69] and the LEGS group quotes $(13.25 \pm 0.86_{-0.58}^{+0.23})10^{-4} fm^3$ [23]. The isospin averaged nucleon polarizabilities determined by MAX-lab measurements of Compton scattering from the deuteron is $(16.4 \pm 3.6)10^{-4} fm^3$ [70]. Running Baldin integrals, with comparisons to MAID, are given in Fig. 11.

The forward spin polarizability γ_0 [71] is

$$\gamma_0 = \frac{1}{4\pi^2} \int_{\nu_0}^{\infty} \frac{\sigma_{1/2} - \sigma_{3/2}}{\nu^3} d\nu. \quad (5)$$

A recent dressed K-matrix model approach for the proton gives $\gamma_0 = -0.9 \cdot 10^{-4} fm^4$ [72]. The LEGS analysis gives, for a proton target, $\gamma_0 = (-1.55 \pm 0.15 \pm 0.003)10^{-4} fm^4$ [23]. The running integral is shown in Fig. 12.

For charge states $\pi^+ n$ and $\pi^- p$, all three quantities are sensitive to the threshold energy range ($E_\gamma < 200$ MeV), as shown in Table VII. From Figs. 10–12, one can see that each integral of the single-pion contribution, based upon the SM02 solution, has essentially converged by 2 GeV.

Experimental data for the GDH and γ_0 quantities have been obtained from measurements at MAMI, covering ranges from 200 to 450 MeV [15] and to 800 MeV [16]. In Tables VIII and IX, we show SM02 and MAID results for the abovementioned quantities over energy ranges corresponding to measurements. Clearly, calculations above 450 MeV have to take into account contributions beyond single-pion photoproduction.

IV. SUMMARY AND CONCLUSION

The single-pion photoproduction database, for proton targets, has increased significantly since the publication of our fit SM95. The inclusion of these precise new measurements has

resulted in a fit with a lower overall χ^2/data . However, some polarization quantities have been difficult to fit, and these difficulties have prompted an examination of the phenomenological forms we use. By changing the way we extrapolate beyond the two-pion threshold, an improved fit was obtained.

This new multipole solution was found to differ significantly from SM95 in a number of partial waves. The largest changes were associated with multipoles connected to πN resonances with $\Gamma_\pi/\Gamma \lesssim 0.3$. Also quite different was the S_{11} multipole, for which the associated πN inelasticity has a sharp increase at the ηN threshold. As might be expected, states with large πN branching fractions remained stable. This stability held for the $N(1520)$ as well, though investigations based upon ηN photoproduction, and quantities related to the GDH integral, have suggested a shift in its ratio of photo-decay amplitudes. Given the sensitivity of weaker resonances to the choice of phenomenology, we are now attempting to replace the dependence on $(\text{Im}T_{\pi N} - T_{\pi N}^2)$ with a form more directly connected to the opening of specific channels, such as ηN and $\pi\Delta$.

The evaluation of sum rules (GDH, Baldin, and forward spin polarizability) for a single-pion contribution exhibits convergence by 2 GeV. Agreement with Mainz is now good below 450 MeV, with larger deviations at higher energies.

In both πN elastic scattering [73] and pion photoproduction [25,39], the measurements of precise new single- and double-polarization data have highlighted problems existing in the “standard” fits. Further polarization measurements will be required to test assumptions implicit in the SAID and MAID programs.

ACKNOWLEDGMENTS

The authors express their gratitude to J. Ahrens, G. Anton, H.-J. Arends, R. Beck, J. C. Bergstrom, J.-P. Bocquet, D. Branford, H. M. Fischer, K. G. Fissum, M. Fuchs, R. Gilman, H. H. Hakopian, D. A. Hutcheon, M. Khandaker, V. Kouznetsov, B. Krusche, B. A. Mecking, A. Omelaenko, P. Pedroni, I. Preobrajenski, D. Rebreyend, G. V. O’Rielly, A. M. Sandorfi, C. Schaerf, and A. Shafi for providing experimental data prior to publication or for clarification of information already published. We also thank L. Tiator and S. Kamalov for the MAID contribution, A. L’vov for a discussion of the sum rules, and A. E. Kudryavtsev for comments on the $S_{11}(1535)$ problem. This work was supported in part by the U. S. Department of Energy under Grant DE-FG02-99ER41110. The authors acknowledge partial support from Jefferson Lab, by the Southeastern Universities Research Association under DOE contract DE-AC05-84ER40150.

REFERENCES

- [1] S. Capstick and W. Roberts, Prog. Part. Nucl. Phys. (Suppl. 2) **45**, 241 (2000).
- [2] R. A. Arndt, I. I. Strakovsky, R. L. Workman, and M. M Pavan, Phys. Rev. C **52**, 2120 (1995).
- [3] R. A. Arndt, I. I. Strakovsky, and R. L. Workman, in: *Proc. of 9th International Symposium on Meson-Nucleon Physics and the Structure of the Nucleon, Washington, DC, USA, July 26–31, 2001*, Eds. H. Haberzettl and W. J. Briscoe, πN Newslett. **16**, 150 (2002), Eprint nucl-th/0110001.
- [4] S. B. Gerasimov, Phys. At. Nucl. (former Sov. J. Nucl. Phys.) **2**, 430 (1966), S. D. Drell and A. C. Hearn, Phys. Rev. Lett. **16**, 908 (1966). For an earlier related work, see L. I. Lapidus and Chou Kuang-chao, JETP (former Sov. J. Phys. JETP) **14**, 357 (1962).
- [5] R. A. Arndt, I. I. Strakovsky, and R. L. Workman, Phys. Rev. C **53**, 430 (1996).
- [6] R. A. Arndt, R. L. Workman, Z. Li, and L. D. Roper, Phys. Rev. C **42**, 1853 (1990); *ibid*, 1864 (1990).
- [7] Z. Li, R. A. Arndt, L. D. Roper, and R. L. Workman, Phys. Rev. C **47**, 2759 (1993).
- [8] The full database and numerous PWAs can be accessed via a ssh/telnet call to the SAID facility gw dac.phys.gwu.edu, with userid: said (no password), or a link to the website <http://gw dac.phys.gwu.edu>.
- [9] M. Fuchs, J. Ahrens, G. Anton, R. Auerbeck, R. Beck, A. M. Bernstein, A. R. Gabler, F. Härter, P. D. Hart, S. Hlavac, B. Krusche, I. J. D. McGregor, V. Metag, R. Novotny, R. O. Owens, J. Peise, M. Röbiger-Landau, A. Schubert, R. S. Simon, H. Ströher, and V. Tries, Phys. Lett. **B368**, 20 (1996), M. Fuchs, Ph. D Theses, University of Giessen, 1995 (unpublished), M. Fuchs, private communication, 1996.
- [10] M. MacCormick, G. Audit, N. d’Hose, L. Ghedira, V. Isbirt, S. Kerhoas, L. Y. Murphy, G. Tamas, P. A. Wallace, S. Altieri, A. Braghieri, P. Pedroni, T. Pinelli, J. Ahrens, R. Beck, J. R. M. Annand, R. A. Crawford, J. D. Kellie, I. J. D. MacGregor, B. Dolbilkin, and A. Zabrodin, Phys. Rev. C **53**, 41 (1996), P. Pedroni, private communication, 1996.
- [11] R. Beck, H. P. Krahn, J. Ahrens, H.-J. Arends, G. Audit, A. Braghieri, N. d’Hose, S. J. Hall, V. Isbert, J. D. Kellie, I. J. D. MacGregor, P. Pedroni, T. Pinelli, G. Tamas, Th. Walcher, and S. Wartenberg, Phys. Rev. Lett. **78**, 606 (1997), H. P. Krahn, Ph. D. Theses, Mainz University, 1996 (unpublished), R. Beck, private communication, 1997.
- [12] F. Härter, Ph. D Theses, Mainz University, KPH15/96, 1996 (unpublished), J. Ahrens, private communication, 2002.
- [13] M. Schneider, Ph. D. Theses, Mainz University, 1994 (unpublished), J. Ahrens, private communication, 1998.
- [14] B. Krusche, J. Ahrens, R. Beck, M. Fuchs, S. J. Hall, F. Härter, J. D. Kellie, V. Metag, M. Röbiger-Landau, and H. Ströher, Eur. Phys. J. A **6**, 309 (1999), B. Krusche, private communication, 1999.
- [15] J. Ahrens, S. Altieri, J. R. M. Annand, G. Anton, H.-J. Arends, K. Aulenbacher, R. Beck, C. Bradtke, A. Braghieri, N. Degrande, N. d’Hose, H. Dutz, S. Görtz, P. Grabmayr, K. Hansen, J. Harmsen, D. von Harrach, S. Hasegawa, T. Hasegawa, E. Heid, K. Helbing, H. Holvoet, L. Van Hoorebeke, N. Horikawa, T. Iwata, P. Jennewein, T. Kageya, B. Kiel, F. Klein, R. Kondratiev, K. Kossert, J. Krimmer, M. Lang, B. Lannoy, R. Leukel, V. Lisin, T. Matsuda, J. C. McGeorge, A. Meier, D. Menze, W. Meyer,

- T. Michel, J. Naumann, R. O. Owens, A. Panzeri, P. Pedroni, T. Pinelli, I. Preobrajenski, E. Radtke, E. Reichert, G. Reicherz, Ch. Rohlof, D. Ryckbosch, F. Sadiq, M. Sauer, B. Schoch, M. Schumacher, B. Seitz, T. Speckner, M. Steigerwald, N. Takabayashi, G. Tamas, A. Thomas, R. van de Vyver, A. Wakai, W. Weihofen, F. Wissmann, F. Zapadtka, and G. Zeitler, Phys. Rev. Lett. **84**, 5950 (2000), H.-J. Arends and I. Preobrajenski, private communication, 2000, P. Pedroni, private communication, 2002.
- [16] J. Ahrens, S. Altieri, J. R. M. Annand, G. Anton, H.-J. Arends, K. Aulenbacher, R. Beck, C. Bradtke, A. Braghieri, N. Degrande, N. d'Hose, H. Dutz, S. Görtz, P. Grabmayr, K. Hansen, J. Harmsen, D. von Harrach, S. Hasegawa, T. Hasegawa, E. Heid, K. Helbing, H. Holvoet, L. Van Hoorebeke, N. Horikawa, T. Iwata, P. Jennewein, T. Kageya, B. Kiel, F. Klein, R. Kondratiev, K. Kossert, J. Krimmer, M. Lang, B. Lannoy, R. Leukel, V. Lisin, T. Matsuda, J. C. McGeorge, A. Meier, D. Menze, W. Meyer, T. Michel, J. Naumann, R. O. Owens, A. Panzeri, P. Pedroni, T. Pinelli, I. Preobrajenski, E. Radtke, E. Reichert, G. Reicherz, Ch. Rohlof, D. Ryckbosch, F. Sadiq, M. Sauer, B. Schoch, M. Schumacher, B. Seitz, T. Speckner, M. Steigerwald, N. Takabayashi, G. Tamas, A. Thomas, R. van de Vyver, A. Wakai, W. Weihofen, F. Wissmann, F. Zapadtka, and G. Zeitler, Phys. Rev. Lett. **87**, 022003 (2001).
- [17] R. Beck, H. P. Krahn, J. Ahrens, J. R. M. Annand, H.-J. Arends, G. Audit, A. Braghieri, N. d'Hose, D. Drechsel, O. Hanstein, J. C. McGeorge, R. O. Owens, P. Pedroni, T. Pinelli, G. Tamas, L. Tiator, and Th. Walcher, Phys. Rev. C **61**, 035204 (2000), H. P. Krahn, Ph. D. Theses, Mainz University, 1996 (unpublished), R. Beck, private communication, 2000.
- [18] D. Branford, J. A. MacKenzie, F. X. Lee, J. Ahrens, J. R. M. Annand, R. Beck, G. E. Cross, T. Davinson, P. Grabmayr, S. J. Hall, P. D. Harty, T. Hehl, D. G. Johnstone, J. D. Kellie, T. Lamparter, M. Liang, I. J. D. MacGregor, J. C. McGeorge, R. O. Owens, M. Sauer, R. Schneider, A. C. Shotter, K. Spaeth, D. P. Watts, P. J. Woods, L. E. Wright, and T. T. Yau, Phys. Rev. C **61**, 014603 (2000), D. Branford, private communication, 2000.
- [19] A. Schmidt, P. Achenbach, J. Ahrens, H.-J. Arends, R. Beck, A. M. Bernstein, V. Hejny, M. Kotulla, B. Krusche, V. Kuhr, R. Leukel, I. J. D. MacGregor, J. C. McGeorge, V. Metag, V. M. Olmos de Leon, F. Rambo, U. Siodlaczek, H. Ströher, Th. Walcher, J. Weiss, F. Wissmann, and M. Wolf, Phys. Rev. Lett. **87**, 232501 (2001), A. Schmidt, Ph. D. Thesis, Mainz University, Sept. 2001 (unpublished), R. Beck, private communication, 2001.
- [20] J. C. Bergstrom, J. M. Vogt, R. Igarashi, K. J. Keeter, E. L. Hallin, G. A. Retzlaff, D. M. Skopik, and E. C. Booth, Phys. Rev. C **53**, 1052 (1996), J. C. Bergstrom, private communication, 1996.
- [21] J. C. Bergstrom, R. Igarashi, and J. M. Vogt, Phys. Rev. C **55**, 2016 (1997), J. C. Bergstrom, private communication, 1997.
- [22] E. Korkmaz, N. R. Kolb, D. A. Hutcheon, G. V. O'Rielly, J. C. Bergstrom, G. Feldman, D. Jordan, A. K. Opper, R. E. Pywell, B. Sawatzky, and D. M. Skopik, Phys. Rev. Lett. **83**, 3609 (1999), G. V. O'Rielly, private communication, 1999.
- [23] G. Blanpied, M. Blecher, A. Caracappa, J. R. Deininger, C. Djalali, G. Giordano, K. Hicks, S. Hoblit, M. Khandaker, O. C. Kistner, A. Kuczewski, F. Lincoln, M. Lowry,

- M. Lucas, G. Matone, L. Miceli, B. M. Preedom, D. Rebreyend, A. M. Sandorfi, C. Schaerf, R. M. Sealock, H. Ströher, C. E. Thorn, S. T. Thornton, J. Tonnison, C. S. Whisnant, H. Zhang, and X. Zhao, *Phys. Rev. C* **64**, 025203 (2001). Differential cross sections for both $\pi^0 p$ and $\pi^+ n$ channels have been flagged.
- [24] J. Ajaka, O. Bartalini, M. Battaglieri, V. Bellini, J.-P. Bocquet, P. M. Calvat, M. Capogni, M. Castoldi, L. Ciciani, A. D'Angelo, J.-P. Didelez, R. Di Salvo, M. A. Duval, C. Gaulard, G. Gervino, F. Ghio, B. Girolami, M. Guidal, E. Guinault, E. Hourany, A. Jejcic, I. Kilvington, V. Kouznetsov, A. Lapik, P. Levi Sandri, A. Lleres, D. Moricciani, V. Nedorezov, L. Nicoletti, D. Rebreyend, F. Renard, M. Ripani, N. Rudnev, C. Schaerf, A. Turinge, and A. Zucchiatti, *Phys. Lett.* **B475**, 372 (2000), V. Kouznetsov, private communication, 2000.
- [25] O. Bartalini, V. Billini, J.-P. Bocquet, M. Capogni, M. Castoldi, A. D'Angelo, J.-P. Didelez, R. Di Salvo, A. Fantini, G. Gervino, F. Ghio, B. Girolami, M. Guidal, E. Hourany, V. Kouznetsov, R. Kunne, A. Lapik, P. Levi Sandri, A. Lleres, D. Moricciani, V. Nedorezov, L. Nicoletti, D. Rebreyend, F. Renard, N. Roudnev, C. Schaerf, M. Sperduto, M. Sutura, A. Turinge, A. Zucchiatti, R. A. Arndt, W. J. Briscoe, I. I. Strakovsky, and R. L. Workman, submitted to *Phys. Lett.* **B**, V. Kouznetsov, private communication, 2001.
- [26] F. V. Adamian, A. Yu. Buniatian, G. S. Frangulian, P. I. Galumian, V. H. Grabski, A. V. Hairapetian, H. H. Hakopian, V. K. Hoktanian, J. V. Manukian, A. M. Sirunian, A. H. Vartapetian, H. H. Vartapetian, V. G. Volchinsky, R. A. Arndt, I. I. Strakovsky, and R. L. Workman, *Phys. Rev. C* **63**, 054606 (2001).
- [27] H. Dutz, D. Kraemer, B. Zucht, K. H. Althoff, G. Anton, H.-J. Arends, W. Beulertz, A. Bock, M. Breuer, R. Gehring, M. Gemander, S. Görtz, K. Helbing, J. Hey, W. Meyer, G. Noldeke, R. Paulsen, G. Reicherz, A. Thomas, and S. Wartenberg, *Nucl. Phys.* **A601**, 319 (1996), G. Anton, private communication, 1996. This is a final version of preliminary T $\pi^+ n$ data used in previous analyses.
- [28] A. Bock, G. Anton, W. Beulertz, Chr. Bradtke, H. Dutz, R. Gehring, S. Görtz, K. Helbing, J. Hey, W. Meyer, M. Pluckthun, G. Reicherz, L. Sözü, M. Breuer, J.-P. Didelez, and P. Hoffmann-Rothe, *Phys. Rev. Lett.* **81**, 534 (1998), G. Anton, private communication, 1996.
- [29] H. W. Dannhausen, E. J. Durwen, H. M. Fischer, M. Leneke, W. Niehaus, and F. Takasaki, *Eur. Phys. J. A* **11**, 441 (2001). This final version of preliminary $\pi^+ n$ differential cross sections by H. W. Dannhausen, Ph. D. Theses, Bonn University, Bonn-IR-77-29, 1977 (unpublished) and M. Leneke, Ph. D. Theses, Bonn University, Bonn-IR-77-14, 1977 (unpublished) used in previous analyses.
- [30] E. J. Durwen, Ph. D. Theses, Bonn University, BONN-IR-80-7, 1980 (unpublished). The final version of these $\pi^+ n$ differential cross sections will submit, H. M. Fischer, private communication, 2001.
- [31] U. Schäfer, Ph. D. Theses, Bonn University, BONN-IR-81-21, 1981 (unpublished). These $\pi^+ n$ differential cross sections have been removed from the database because they were taken in a first test of a new spectrometer, H. M. Fischer, private communication, 2001.
- [32] W. Heise, Ph. D. Theses, Bonn University, BONN-IR-88-06, 1988 (unpublished). The final version of these $\pi^+ n$ differential cross sections will submit, H. M. Fischer, private

- communication, 2001.
- [33] P. Zenz, Ph. D. Theses, Bonn University, BONN-IR-88-12, 1988 (unpublished). The final version of these $\pi^0 p$ differential cross sections will submit, H. M. Fischer, private communication, 2001.
 - [34] W. J. Briscoe, J. Ficenec, D. Jenkins *et al.* CEBAF Proposal, E-94-103, 1994.
 - [35] I. Preobrajenski, in: *Proc. of 9th International Symposium on Meson-Nucleon Physics and the Structure of the Nucleon, Washington, DC, USA, July 26-31, 2001*, Eds. H. Haberzettl and W. J. Briscoe, πN Newslett. **16**, 308 (2001), I. Preobrajenski, Ph. D. Thesis, Mainz University, Sept. 2001 (unpublished).
 - [36] I. S. Barker, A. Donnachie, and J. K. Storrow, Nucl. Phys. **B95**, 347 (1975).
 - [37] R. Leukel, Ph. D. Thesis, Mainz University, Sept. 2001 (unpublished).
 - [38] D. Rebreyend, private communication, 1999.
 - [39] R. J. Holt, R. Gilman *et al.* CEBAF Proposal, E-94-012, 1994, R. Gilman, private communication, 2000.
 - [40] A. M. Sandorfi, private communication, 1995. The preliminary version of $\pi^- p \Sigma$ has been used in previous analyses.
 - [41] A. Shafi for the Crystal Ball Collaboration, Bull. Am. Phys. Soc. **44**, 43 (1999).
 - [42] K. Watson, Phys. Rev. **95**, 228 (1954).
 - [43] R. A. Arndt, R. L. Workman, I. I. Strakovsky, and M. M. Pavan, in preparation, Eprint nucl-th/9807087, <http://gwdac.phys.gwu.edu>.
 - [44] Mainz fits are available at the MAID website <http://www.kph.uni-mainz.de/MAID/>. See also S. S. Kamalov, S. N. Yang, D. Drechsel, O. Hanstein, and L. Tiator, Phys. Rev. C **64**, 032201 (2001). The Unitary Isobar Model is developed at Mainz (hereafter called MAID), D. Drechsel, O. Hanstein, S. S. Kamalov, and L. Tiator, Nucl. Phys. **A645**, 145 (1999). MAID2000 refers to the Feb. 2001 version of the MAID solution, MAID2001 refers to the Nov. 2001 version of the MAID solution from S. Kamalov.
 - [45] J. Ahrens, S. Altieri, J. R. M. Annand, G. Anton, H.-J. Arends, K. Aulenbacher, R. Beck, C. Bradtke, A. Braghieri, N. Degrande, N. d'Hose, D. Drechsel, H. Dutz, S. Görtz, P. Grabmayr, K. Hansen, J. Harmsen, D. von Harrach, S. Hasegawa, T. Hasegawa, E. Heid, K. Heibling, H. Holvöt, L. Van Hoorebeke, N. Norikawa, T. Iwata, O. Jahn, P. Jennewein, T. Kageya, S. Kamalov, B. Kiel, F. Klein, R. Kondratiev, K. Kossert, J. Krimmer, M. Lang, B. Lannoy, R. Leukel, V. Lisin, T. Matsuda, J. C. McGeorge, A. Meier, D. Menze, W. Meyer, T. Michel, J. Naumann, A. Panzeri, P. Pedroni, T. Pinelli, I. Preobrajenski, E. Radtke, E. Reichert, G. Reicherz, Ch. Rohlof, G. Rosner, D. Ryckbosch, M. Sauer, B. Schoch, M. Schumacher, B. Seitz, T. Speckner, N. Takabayashi, G. Tamas, A. Thomas, L. Tiator, R. van de Vyver, A. Wakai, W. Weihofen, F. Wissmann, F. Zapadtka, and G. Zeitler, Eprint hep-ex/0203006, submitted to Phys. Rev. Lett. This set is a part of Ref. [35] and has not been used in our analysis.
 - [46] R. A. Arndt, I. Aznauryan, R. M. Davidson, D. Drechsel, O. Hanstein, S. S. Kamalov, A. S. Omelaenko, I. I. Strakovsky, L. Tiator, R. L. Workman, and S. N. Yang, Summary of the Partial Wave Analysis Group of the BRAG workshop, Mainz, March 5-6, 2001, in: *Proceedings of NSTAR2001, Mainz, Germany, March 7-10, 2001*, Eds. D. Drechsel and L. Tiator, World Scientific, p. 467; Eprint nucl-th/0106059.
 - [47] S. S. Kamalov, G.-Y. Chen, S. N. Yang, D. Drechsel, and L. Tiator, Phys. Lett. **B522**, 27 (2001).

- [48] O. Hanstein, D. Drechsel, and L. Tiator, Phys. Lett. **B385**, 45 (1996).
- [49] P. J. Bussey, C. Raine, J. G. Rutherglen, P. S. L. Booth, L. J. Carroll, G. R. Court, P. R. Daniel, A. W. Edwards, R. Gamet, C. J. Hardwick, P. J. Hayman, J. R. Holt, J. N. Jackson, J. H. Norem, W. H. Range, F. H. Combley, W. Galbraith, V. H. Rajaratnam, and C. Sutton, Nucl. Phys. **B154**, 205 (1979).
- [50] J. Alspector, D. Fox, D. Luckey, C. Nelson, L. S. Osborne, G. Tarnopolsky, Z. Bar-Yam, J. De Pagter, J. Dowd, W. Kern, and S. M. Matin, Phys. Rev. Lett. **28**, 1403 (1972).
- [51] C. Betourne, J. C. Bizot, J. P. Perez-y-Jorba, D. Treille, and W. Schmidt, Phys. Rev. **172**, 1343 (1968).
- [52] S. D. Ecklund and R. L. Walker, Phys. Rev. **159**, 1195 (1967).
- [53] J. H. Boyden, Ph. D. Thesis, UCLA, 1961 (unpublished).
- [54] J. R. Kilner, Ph. D. Thesis, UCLA, 1962 (unpublished).
- [55] G. Buschhorn, J. Carroll, R. D. Eandi, P. Heide, R. Hübner, W. Kern, U. Kötz, P. Schmüser, and H. J. Skronn, Phys. Rev. Lett. **18**, 571 (1967).
- [56] D. Sober, <http://www.jlab.org/~sober/GDH/>
- [57] G. Zeitler, in: *Proc. of 9th International Symposium on Meson-Nucleon Physics and the Structure of the Nucleon, Washington, DC, USA, July 26–31, 2001*, Eds. H. Haberzettl and W. J. Briscoe, *πN Newslett.* **16**, 311 (2001).
- [58] T. Iwata, in: *Proc. of the Gerasimov-Drell-Hearn Sum Rule and the Nucleon Spin Structure in the Resonance Region, Mainz, Germany, June 14–17, 2000*, Eds. D. Drechsel and L. Tiator, p. 289, <http://kiso.phys.nagoya-u.ac.jp/~iwata/publication.html>.
- [59] A. Lehman, *Proceedings of 9th International Conference on the Structure of Baryons (BARYONS2002), Newport News, VA, USA, March 3–8, 2002*, to be published.
- [60] L. Tiator, talk given at 9th International Symposium on Meson-Nucleon Physics and the Structure of the Nucleon, Washington, DC, USA, July 26–31, 2001, private communication, 2001.
- [61] S. S. Kamalov, private communication, 2002.
- [62] R. L. Crawford and W. T. Morton, Nucl. Phys. **B211**, 1 (1983), Particle Data Group, Phys. Lett. **B239**, 1 (1990).
- [63] R. L. Crawford, in: *Proceedings of NSTAR2001, Mainz, Germany, March 7–10, 2001*, Eds. D. Drechsel and L. Tiator, World Scientific, p. 163.
- [64] D. Drechsel, O. Hanstein, S. S. Kamalov, and L. Tiator, Nucl. Phys. **A645**, 145 (1999).
- [65] D. E. Groom *et al.*, *Review of Particle Physics*, Eur. Phys. J. C **15**, 1 (2000), 2001 off-year partial update for 2002 edition available on the PDG site <http://pdg.lbl.gov>.
- [66] S. Capstick, Phys. Rev. D **46**, 2864 (1992).
- [67] A. M. Baldin, Nucl. Phys. **18**, 310 (1960), L. I. Lapidus, JETP (former Sov. J. Phys. JETP) **16**, 964 (1963).
- [68] M. I. Levchuk and A. I. L'vov, Nucl. Phys. **A674**, 449 (2000).
- [69] V. Olmos de Leon, F. Wissmann, P. Achenbach, J. Ahrens, H. J. Arends, R. Beck, P. D. Harty, V. Hejny, P. Jennewein, M. Kotulla, B. Krusche, V. Kuhr, R. Leukel, J. C. McGeorge, V. Metag, R. Novotny, A. Polonski, F. Rambo, A. Schmidt, M. Schumacher, U. Siodlaczek, H. Ströher, A. Thomas, J. Weiss, and M. Wolf, Eur. Phys. J. A **10**, 207 (2001).
- [70] M. Lundin, J.-O. Adler, T. Glebe, K. Fissum, K. Hansen, L. Isaksson, O. Kaltschmidt,

- M. Karlsson, K. Kossert, M. I. Levchuk, P. Lilja, B. Lindner, A. I. L'vov, B. Nilsson, D. E. Oner, C. Poech, S. Proff, A. Sandell, B. Schröder, M. Schumacher, and D. A. Sims, Eprint nucl-ex/0204014, submitted to Phys. Rev. Lett.
- [71] S. Ragusa, Phys. Rev. D **47**, 3757 (1993).
- [72] S. Kondratyuk and O. Scholten, Phys. Rev. C **65**, 038201 (2002).
- [73] I. G. Alekseev, V. P. Kanavets, B. V. Morozov, D. N. Svirida, S. P. Kruglov, A. A. Kulbardin, V. V. Sumachev, R. A. Arndt, I. I. Strakovsky, and R. L. Workman, Phys. Rev. C **55**, 2049 (1997).

TABLES

TABLE I. Comparison of present (SM02) and previous (SM95 [5], SP93 [7], and SP89 [6]) energy-dependent partial-wave analyses of charged and neutral pion photoproduction data. The χ^2 values for the previous solutions correspond to our published results. N_{prm} is the number parameters varied in the fit.

Solution	Range (MeV)	$\chi^2/\pi^0 p$	$\chi^2/\pi^+ n$	$\chi^2/\pi^- p$	$\chi^2/\pi^0 n$	N_{prm}
SM02	2000	18686/8092	12246/7279	4123/2080	241/120	148
SM95	2000	13087/4711	12284/6359	6156/2225	282/120	135
SP93	1800	14093/4015	22426/6019	8280/2312	275/120	134
SP89	1000	13073/3241	11092/3847	4947/1728	461/120	97

TABLE II. Comparison of χ^2/data for normalized (Norm) and unnormalized (Unnorm) data for SM02 solution.

Data	Norm	Unnorm
$\pi^0 p$	2.3	3.8
$\pi^+ n$	1.7	2.7
$\pi^- p$	2.0	2.6
$\pi^0 n$	2.0	2.0

TABLE III. Comparison of χ^2/data for the SM02 solution over the 600–900 MeV range, associated with the N(1535), versus full database and more recent measurements.

Reaction	Observable	All	1980–Present	1985–Present
$\pi^0 p$	$d\sigma/d\Omega$	3946/1644	1808/992	1211/903
	Σ	479/179	345/122	277/105
	P	361/181	177/103	56/33
	T	376/72	2/2	2/2
$\pi^+ n$	$d\sigma/d\Omega$	1343/1407	768/930	349/596
	Σ	954/251	594/134	565/112
	P	158/62	5/5	—
	T	437/228	44/60	44/60

TABLE IV. Single-energy (binned) fits of combined charge and neutral pion photoproduction data, with χ^2 values. N_{prm} is the number parameters varied in the single-energy fits, and χ_E^2 is given by the energy-dependent fit, SM02, over the same energy interval.

E_γ (MeV)	Range (MeV)	N_{prm}	χ^2/data	χ_E^2	E_γ (MeV)	Range (MeV)	N_{prm}	χ^2/data	χ_E^2
152	148 – 155	5	494/269	596	885	873 – 896	28	210/161	374
157	153 – 160	5	463/240	596	905	893 – 916	28	461/329	740
162	158 – 165	5	370/211	401	925	913 – 936	28	139/149	293
167	163 – 170	5	422/173	540	945	933 – 956	29	476/263	704
172	168 – 175	5	116/ 86	157	965	953 – 975	20	145/130	280
177	173 – 180	5	136/105	148	985	973 – 996	20	130/130	227
182	178 – 185	5	149/105	174	1005	993 – 1016	29	508/294	766
187	183 – 190	5	69/ 99	124	1025	1013 – 1037	20	230/131	313
192	188 – 195	10	124/133	153	1045	1033 – 1057	29	256/205	417
197	193 – 200	5	131/105	154	1065	1053 – 1076	29	126/124	191
202	199 – 205	5	128/ 95	157	1085	1073 – 1096	29	92/ 97	155
207	203 – 210	5	154/111	173	1105	1093 – 1115	29	359/212	479
212	208 – 215	10	184/148	223	1125	1114 – 1136	29	139/ 98	224
217	213 – 220	9	182/138	297	1145	1133 – 1155	29	212/160	328
222	218 – 225	15	239/178	367	1165	1153 – 1176	21	110/ 98	167
227	223 – 230	15	124/148	188	1185	1173 – 1194	21	54/ 73	98
232	228 – 235	15	230/176	254	1205	1193 – 1216	29	218/185	314
237	233 – 240	15	266/215	306	1225	1213 – 1236	11	98/ 83	149
242	238 – 245	15	319/218	398	1245	1233 – 1255	29	116/118	217
247	243 – 250	15	352/211	472	1265	1253 – 1276	21	65/ 67	129
265	253 – 276	15	1371/698	1641	1285	1273 – 1297	11	34/ 45	68
285	273 – 297	16	1060/491	1207	1305	1293 – 1315	21	275/139	435
305	293 – 316	16	898/492	957	1325	1313 – 1335	11	42/ 48	79
325	313 – 336	16	1124/473	1344	1345	1334 – 1355	21	178/102	262
345	333 – 356	16	823/532	1043	1365	1354 – 1376	11	41/ 40	62
365	353 – 376	16	579/443	799	1385	1374 – 1395	11	59/ 36	81
385	373 – 396	17	450/406	587	1405	1394 – 1416	21	324/147	509
405	393 – 416	18	639/448	785	1425	1414 – 1436	21	53/ 57	110
425	413 – 436	18	497/358	654	1445	1434 – 1456	21	89/ 91	147
445	433 – 456	18	409/275	524	1465	1453 – 1475	11	62/ 36	100
465	453 – 476	18	298/230	345	1485	1473 – 1495	11	64/ 35	95
485	473 – 496	19	284/192	405	1505	1493 – 1515	21	107/ 98	198
505	493 – 516	19	430/272	517	1525	1514 – 1536	11	74/ 37	103
525	513 – 536	20	223/202	285	1545	1533 – 1555	11	46/ 53	63
545	533 – 556	20	348/237	336	1565	1554 – 1575	11	11/ 19	30
565	553 – 577	20	311/211	369	1585	1574 – 1595	21	42/ 34	73
585	573 – 596	20	432/275	560	1605	1593 – 1616	21	90/ 87	146
605	593 – 616	20	318/286	406	1625	1613 – 1635	11	40/ 24	77
625	613 – 636	20	384/294	482	1645	1634 – 1655	11	118/ 73	149
645	633 – 656	20	469/332	583	1665	1654 – 1675	21	24/ 36	36
665	653 – 676	21	528/405	637	1685	1673 – 1695	11	25/ 31	34

685	673 – 696	21	647/436	795	1705	1693 – 1715	21	98/ 88	139
705	693 – 716	21	1112/625	1219	1725	1714 – 1735	11	10/ 15	19
725	713 – 736	26	425/402	620	1745	1734 – 1755	11	101/ 42	121
745	733 – 757	26	932/580	1179	1765	1753 – 1775	11	53/ 35	57
765	753 – 776	26	552/400	787	1785	1774 – 1796	11	25/ 21	36
785	773 – 797	26	470/387	699	1805	1794 – 1815	21	78/ 70	129
805	793 – 816	27	510/347	758	1845	1824 – 1865	11	125/ 67	155
825	813 – 836	27	243/183	332	1900	1879 – 1920	21	158/ 99	212
845	833 – 856	27	542/338	761	1990	1969 – 2005	21	150/100	326
865	853 – 876	27	164/150	280					

TABLE V. Comparison of χ^2 for the SM95 [5], SM02, and SX99 solutions to 2 GeV versus the present database. Only a fraction of this database was used in generating SM95.

Reaction	Observable	SM95	SM02	SX99	Data
$\pi^0 p$	$d\sigma/d\Omega$	32235	12681	12745	5523
	σ_{tot}	1577	1331	1681	713
	$\sigma_{1/2} - \sigma_{3/2}$	7	10	10	13
	Σ	3238	1918	1975	772
	P	1269	1390	1393	576
	T	1499	1651	1678	389
$\pi^+ n$	$d\sigma/d\Omega$	7587	6364	6952	4995
	σ_{tot}	132	70	84	76
	$\sigma_{1/2} - \sigma_{3/2}$	147	29	67	13
	Σ	8672	2881	3780	1047
	P	512	471	430	250
	T	1678	1512	1854	694
$\pi^- p$	$d\sigma/d\Omega$	3702	3098	3118	1570
	σ_{tot}	227	157	165	117
	Σ	541	600	576	216
	P	159	144	161	88
	T	117	157	129	96

TABLE VI. Resonance couplings from a Breit-Wigner fit to the SM02 solution [GW] and SES [GWSES] (to illustrate the difference, we include $D_{35}(1930)$ and $D_{37}(1950)$ twice, once with the GWSES database and once with the GW (global fit) database), our previous solution SM95 [VPI] [5], the analysis of Crawford and Morton [CM83] [62], Crawford [CR01] [63], Drechsel *et al.* [MAID98] [64], an average from the Particle Data Group [PDG] [65], and quark model predictions of Capstick [CAP92] [66].

Resonance State	Reference	$\gamma p (GeV)^{-1/2} * 10^{-3}$		$\gamma n (GeV)^{-1/2} * 10^{-3}$	
		$A_{1/2}$	$A_{3/2}$	$A_{1/2}$	$A_{3/2}$
S₁₁(1650)	GWSES	74 ± 1		-28 ± 4	
$W_R = 1674 \text{ MeV}$	VPI	69 ± 5		-15 ± 5	
$\Gamma_\pi/\Gamma = 0.77$	CM83	33 ± 15		-68 ± 40	
$\Gamma = 191 \text{ MeV}$	CR01	71		—	
	MAID98	39		-32	
	PDG	53 ± 16		-15 ± 21	
	CAP92	54		-35	
P₁₁(1440)	GWSES	-67 ± 2		47 ± 5	
$W_R = 1472 \text{ MeV}$	VPI	-63 ± 5		45 ± 15	
$\Gamma_\pi/\Gamma = 0.64$	CM83	-69 ± 18		56 ± 15	
$\Gamma = 434 \text{ MeV}$	CR01	-88		—	
	MAID98	-71		60	
	PDG	-65 ± 4		40 ± 10	
	CAP92	4		-6	
D₁₃(1520)	GWSES	-24 ± 2	135 ± 2	-67 ± 4	-112 ± 3
$W_R = 1517 \text{ MeV}$	VPI	-20 ± 7	167 ± 5	-48 ± 8	-140 ± 10
$\Gamma_\pi/\Gamma = 0.63$	CM83	-28 ± 14	156 ± 22	-56 ± 11	-144 ± 15
$\Gamma = 109 \text{ MeV}$	CR01	-15	162	—	—
	MAID98	-17	164	-40	-135
	PDG	-24 ± 9	166 ± 5	-59 ± 9	-139 ± 11
	CAP92	-15	134	-38	-114
D₁₅(1675)	GWSES	33 ± 4	9 ± 3	-50 ± 4	-71 ± 5
$W_R = 1678 \text{ MeV}$	VPI	15 ± 10	10 ± 7	-49 ± 10	-51 ± 10
$\Gamma_\pi/\Gamma = 0.39$	CM83	21 ± 11	15 ± 9	-59 ± 15	-59 ± 20
$\Gamma = 144 \text{ MeV}$	CR01	13	38	—	—
	MAID98	—	—	—	—
	PDG	19 ± 8	15 ± 9	-43 ± 12	-58 ± 13
	CAP92	2	3	-35	-51
F₁₅(1680)	GWSES	-13 ± 2	129 ± 2	29 ± 6	-58 ± 9
$W_R = 1682 \text{ MeV}$	VPI	-10 ± 4	145 ± 5	30 ± 5	-40 ± 15
$\Gamma_\pi/\Gamma = 0.68$	CM83	-17 ± 18	132 ± 10	44 ± 12	-33 ± 15
$\Gamma = 120 \text{ MeV}$	CR01	-14	135	—	—
	MAID98	-10	138	35	-41

	PDG	-15 ± 6	133 ± 12	29 ± 10	-33 ± 9
	CAP92	-38	56	19	-23
S₃₁(1620)	GWSES	-13 ± 3			
$W_R = 1612 \text{ MeV}$	VPI	35 ± 20			
$\Gamma_\pi/\Gamma = 0.34$	CM83	35 ± 10			
$\Gamma = 117 \text{ MeV}$	CR01	17			
	MAID98	$-$			
	PDG	27 ± 11			
	CAP92	81			
P₃₃(1232)	GWSES	-129 ± 1	-243 ± 1		
$W_R = 1235 \text{ MeV}$	VPI	-141 ± 5	-261 ± 5		
$\Gamma_\pi/\Gamma = 1.00$	CM83	-145 ± 15	-263 ± 26		
$\Gamma = 119 \text{ MeV}$	CR01	-149	-259		
	MAID98	-138	-256		
	PDG	-135 ± 6	-255 ± 8		
	CAP92	-108	-186		
D₃₃(1700)	GWSES	89 ± 10	92 ± 7		
$W_R = 1668 \text{ MeV}$	VPI	90 ± 25	97 ± 20		
$\Gamma_\pi/\Gamma = 0.16$	CM83	111 ± 17	107 ± 15		
$\Gamma = 300 \text{ MeV}$	CR01	79	90		
	MAID98	86	85		
	PDG	104 ± 15	85 ± 22		
	CAP92	82	68		
D₃₅(1930)	GWSES	4 ± 6	-3 ± 6		
$W_R = 2113 \text{ MeV}$	GW	6 ± 2	-4 ± 2		
$\Gamma_\pi/\Gamma = 0.14$	VPI	-7 ± 10	5 ± 10		
$\Gamma = 524 \text{ MeV}$	CM83	-38 ± 47	-23 ± 80		
	CR01	8	8		
	MAID98	$-$	$-$		
	PDG	-9 ± 28	-18 ± 28		
	CAP92	$-$	$-$		
F₃₅(1905)	GWSES	2 ± 5	-56 ± 5		
$W_R = 1845 \text{ MeV}$	VPI	22 ± 5	-45 ± 5		
$\Gamma_\pi/\Gamma = 0.13$	CM83	21 ± 10	-56 ± 28		
$\Gamma = 300 \text{ MeV}$	CR01	17	-18		
	MAID98	$-$	$-$		
	PDG	26 ± 11	-45 ± 20		
	CAP92	26	-1		
F₃₇(1950)	GWSES	-62 ± 4	-80 ± 3		

$W_R = 1929 \text{ MeV}$	GW	-64 ± 4	-83 ± 4
$\Gamma_\pi/\Gamma = 0.49$	VPI	-79 ± 6	-103 ± 6
$\Gamma = 274 \text{ MeV}$	CM83	-67 ± 14	-82 ± 17
	CR01	-59	-62
	MAID98	$-$	$-$
	PDG	-76 ± 12	-97 ± 10
	CAP92	-33	-42

TABLE VII. Comparison of the SM02 and recent MAID2000 [44] calculations for the GDH and Baldin integrals and the forward spin polarizability from threshold to 2 GeV (for MAID to 1.25 GeV) [upper set] and from threshold to 200 MeV [lower set] displayed as SAID/MAID.

Reaction	GDH (μb)	Baldin ($10^{-4} fm^3$)	γ_0 ($10^{-4} fm^4$)
$\pi^0 p$	$-142/-150$	$4.7/4.7$	$-1.40/-1.47$
$\pi^+ n$	$-45/-18$	$6.8/6.9$	$0.55/ 0.79$
$\pi^0 n$	$-148/-153$	$4.6/4.6$	$-1.44/-1.50$
$\pi^- p$	$11/ 33$	$8.3/8.8$	$1.36/ 1.64$
$\pi^0 p$	$-2/-1$	$0.1/0.1$	$-0.05/-0.04$
$\pi^+ n$	$30/ 32$	$1.2/1.2$	$0.99/ 1.02$
$\pi^0 n$	$-1/-1$	$0.1/0.1$	$-0.04/-0.04$
$\pi^- p$	$42/ 47$	$1.7/1.8$	$1.39/ 1.53$

TABLE VIII. Comparison of the SM02 and recent MAID2000 [44] calculations, and recent Mainz data [15] for the GDH and Baldin integrals and the forward spin polarizability for proton and neutron targets from 200 to 450 MeV. Units are μb , $10^{-4} fm^3$, and $10^{-4} fm^4$ for the GDH and Baldin integrals and polarizability, respectively.

Integral	Reaction	SAID	MAID	Mainz
GDH	$\pi^0 p$	-129	-136	$-144 \pm 7 \pm 9$
	$\pi^+ n$	-42	-25	$-32 \pm 3 \pm 2$
	proton	-171	-161	$-176 \pm 8 \pm 11$
	$\pi^- p$	-14	-1	
	$\pi^0 n$	-135	-139	
	neutron	-149	-140	
Baldin	$\pi^0 p$	4.0	4.0	
	$\pi^+ n$	4.5	4.6	
	proton	8.5	8.6	
	$\pi^- p$	5.5	5.9	
	$\pi^0 n$	3.9	4.0	
	neutron	9.5	9.8	
γ_0	$\pi^0 p$	-1.31	-1.39	$-1.45 \pm 0.09 \pm 0.09$
	$\pi^+ n$	-0.39	-0.21	$-0.23 \pm 0.04 \pm 0.01$
	proton	-1.71	-1.61	$-1.68 \pm 0.10 \pm 0.10$
	$\pi^- p$	-0.05	0.11	
	$\pi^0 n$	-1.35	-1.40	
	neutron	-1.41	-1.29	

TABLE IX. Comparison of the SM02 and recent MAID2000 [44] calculations, and recent Mainz data [16] for the GDH and Baldin integrals and the forward spin polarizability for proton and neutron targets from 200 to 800 MeV. Units are μb , $10^{-4} fm^3$, and $10^{-4} fm^4$ for the GDH and Baldin integrals and polarizability, respectively.

Integral	Reaction	SAID	MAID	Mainz
GDH	proton	-193	-175	$-226 \pm 5 \pm 12$
	neutron	-167	-160	
Baldin	proton	9.8	9.9	
	neutron	10.9	11.3	
γ_0	proton	-1.76	-1.63	$-1.87 \pm 0.08 \pm 0.10$
	neutron	-1.46	-1.34	

Figure captions

Figure 1. Energy-angle distribution of recent (post-1995) data: (a) unpolarized $\pi^0 p$, (b) polarized $\pi^0 p$, (c) unpolarized $\pi^+ n$, (d) polarized $\pi^+ n$. (a,c) total cross sections and (b,d) $(\sigma_{1/2} - \sigma_{3/2})$ are plotted at zero degrees.

Figure 2. Partial-wave amplitudes ($L_{2I,2J}$) from threshold to $E_\gamma = 2$ GeV. Solid (dashed) curves give the real (imaginary) parts of amplitudes corresponding to the SM02 solution. The real (imaginary) parts of single-energy solutions are plotted as filled (open) circles. The previous SM95 solution [5] is plotted with long dash-dotted (real part) and short dash-dotted (imaginary part) lines. Plotted are the multipole amplitudes (a) ${}_pE_{0+}^{1/2}$, (b) ${}_nE_{0+}^{1/2}$, (c) ${}_pE_{0+}^{3/2}$, (d) ${}_pM_{1-}^{1/2}$, (e) ${}_nM_{1-}^{1/2}$, (f) ${}_pE_{1+}^{1/2}$, (g) ${}_pM_{1+}^{1/2}$, (h) ${}_nE_{1+}^{1/2}$, (i) ${}_nM_{1+}^{1/2}$, (j) ${}_pM_{1-}^{3/2}$, (k) ${}_pE_{1+}^{3/2}$, (l) ${}_pM_{1+}^{3/2}$, (m) ${}_pE_{2-}^{1/2}$, (n) ${}_pM_{2-}^{1/2}$, (o) ${}_nE_{2-}^{1/2}$, (p) ${}_nM_{2-}^{1/2}$, (q) ${}_pE_{2-}^{3/2}$, (r) ${}_pE_{2+}^{3/2}$, (s) ${}_pE_{3-}^{1/2}$, (t) ${}_pM_{3-}^{1/2}$, (u) ${}_nE_{3-}^{1/2}$, (v) ${}_nM_{3-}^{1/2}$, (w) ${}_pE_{3-}^{3/2}$, and (x) ${}_pM_{3+}^{3/2}$. The subscript p (n) denotes a proton (neutron) target.

Figure 3. Differential cross section $(d\sigma/d\Omega_{1/2} - d\sigma/d\Omega_{3/2})$ for $\vec{\gamma}\vec{p} \rightarrow \pi^0 p$ at $\theta = 85 \pm 4^\circ$. The solid (dash-dotted) line plots the SM02 (MAID2001 [44]) solution. Experimental data are from Mainz [45].

Figure 4. Photon asymmetry for π^0 photoproduction on the proton at 159.5 MeV. Data are from Mainz (solid circles) [19]. Plotted are the SM02 (solid line), the 162 MeV-SES (158 – 165 MeV) fit associated with SM02 (dotted lines represent uncertainties of the SES fit) and the MAID2000 results (dash-dotted) [44].

Figure 5. Σ beam asymmetry for $\pi^+ n$ at 1100 MeV. Black circles show GRAAL results [25], open circles indicate the results of the Daresbury group [49], open triangles indicate the results from Saclay [50]. The solid (dash-dotted) line represents the SM02 (MAID2001 [44]) solution.

Figure 6. Forward (5°) differential cross section for $\gamma p \rightarrow \pi^+ n$ as a function of energy. Experimental data for the range of $5 \pm 2^\circ$ are from Orsay [51] (black circles), SLAC [52] (open circles), [53] (open triangles), [54] (black square), and DESY [55] (black diamonds.) The solid (dash-dotted) line represents the SM02 (MAID2001 [44]) solution.

Figure 7. Difference of the total cross sections for the helicity states 1/2 and 3/2. (a) $\vec{\gamma}\vec{p} \rightarrow \pi^0 p$ and (b) $\vec{\gamma}\vec{p} \rightarrow \pi^+ n$. The solid (dash-dotted) line represents the SM02 (MAID2001 [44]) solution. Experimental data are from Mainz [15].

Figure 8. Selected partial-wave amplitudes to $E_\gamma = 1250$ MeV. Solid (dashed) curves give the real (imaginary) parts of amplitudes corresponding to the SM02 solution. The recent MAID2001 solution [44] is plotted with long dash-dotted (real part) and short dash-dotted (imaginary part) lines. Plotted are the multipole amplitudes (a) $S_{11}pE$ [${}_pE_{0+}^{1/2}$], (b) $P_{13}pE$ [${}_pE_{1+}^{1/2}$], (c) $P_{31}pM$ [${}_pM_{1-}^{3/2}$], and (d) $D_{13}pE$ [${}_pE_{2-}^{1/2}$]. The subscript p (n) denotes a proton (neutron) target.

Figure 9. $S_{11}pE$ multipole for 600 to 1200 MeV. Plotted are (a) real part and (b) imaginary part. The SM02 (SX99) solution is plotted with a solid (dashed) line and previous SM95 solution [5] with a dash-dotted line.

Figure 10. Running GDH integral. (a) for proton and (b) neutron targets. The solid (dash-dotted) line represents the SM02 (MAID2000 [44]) solution.

Figure 11. Running Baldin integral. (a) for proton and (b) neutron targets. The solid (dash-dotted) line represents the SM02 (MAID2000 [44]) solution.

Figure 12. Forward spin polarizability γ_0 . (a) for proton and (b) neutron targets. The solid (dash-dotted) line represents the SM02 (MAID2000 [44]) solution.

FIGURES

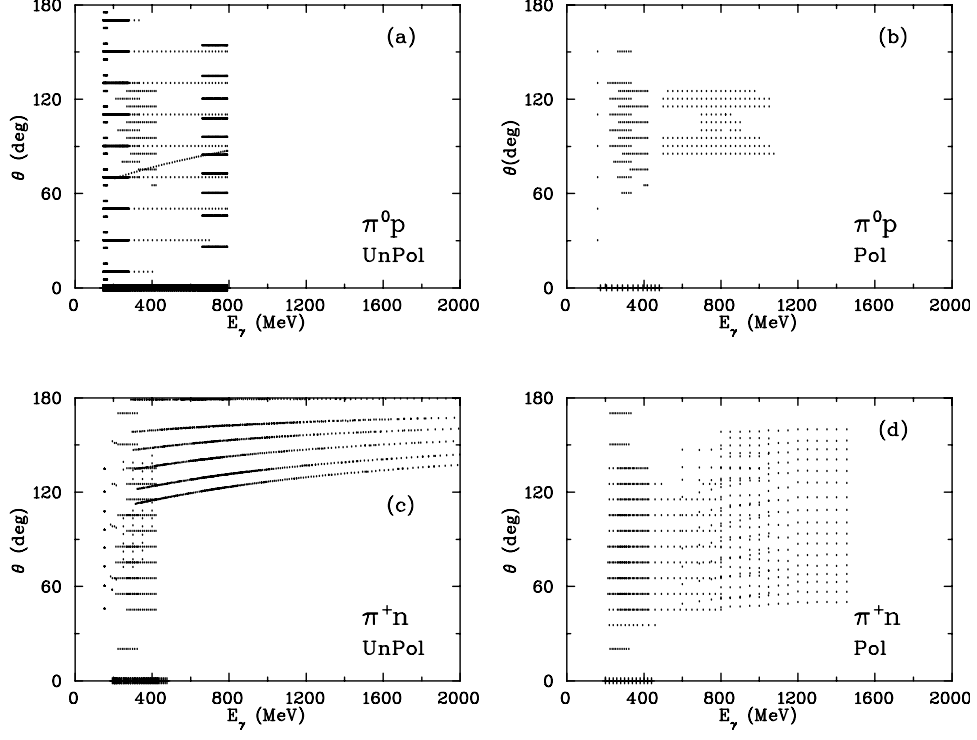
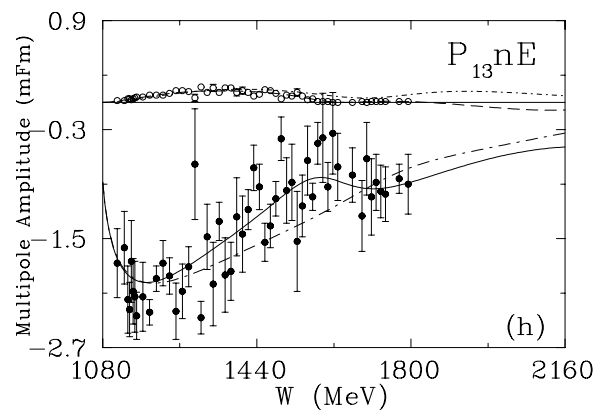
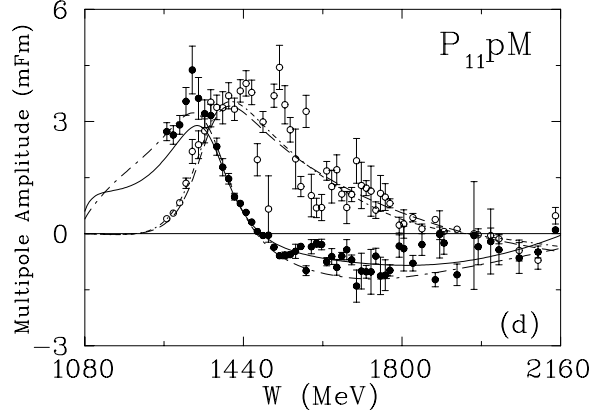
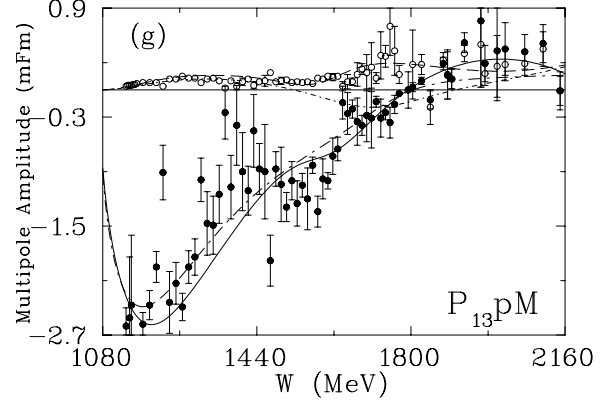
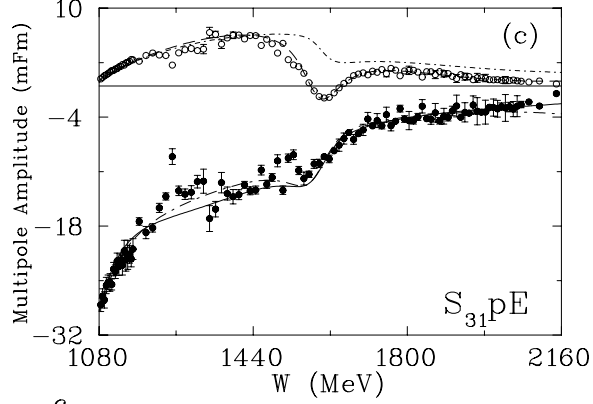
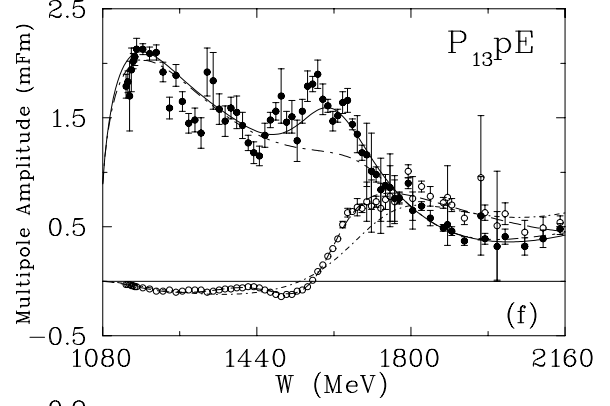
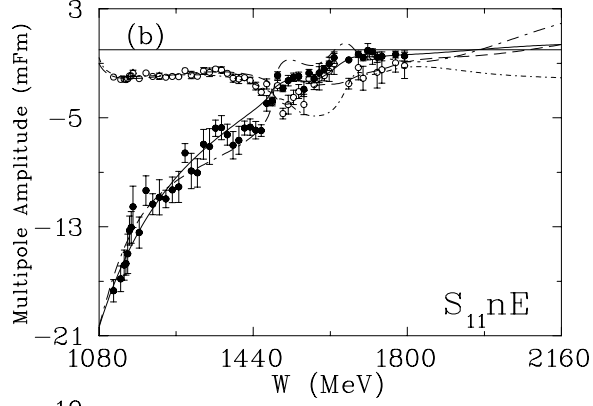
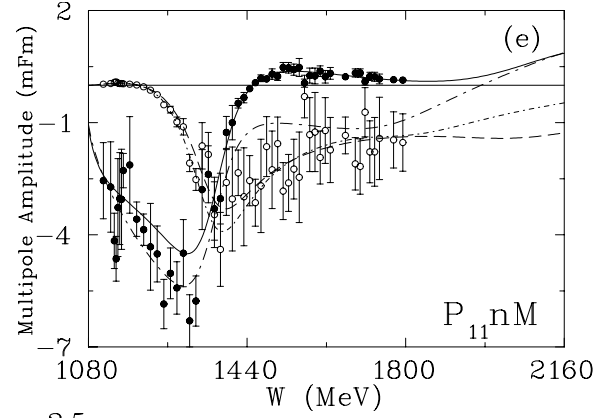
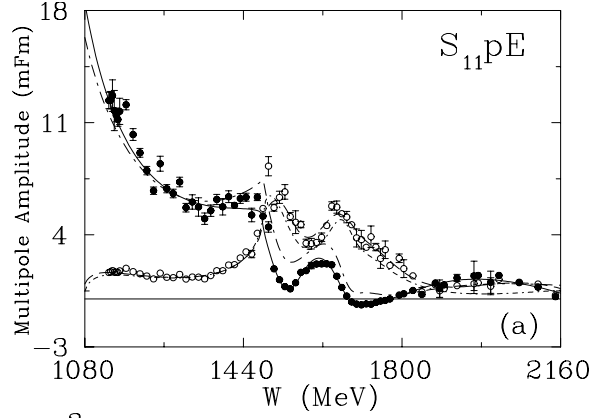
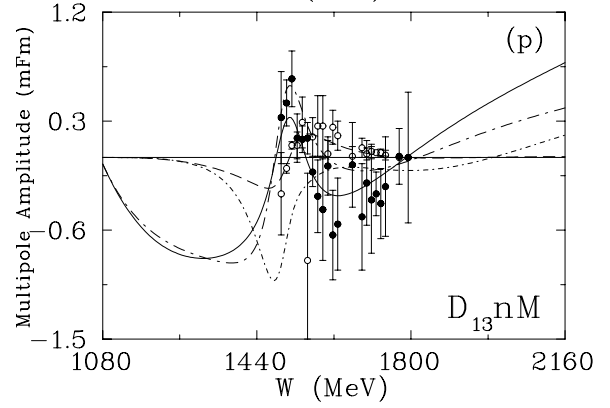
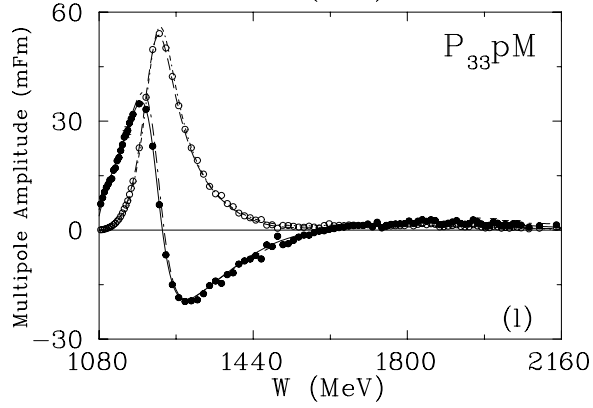
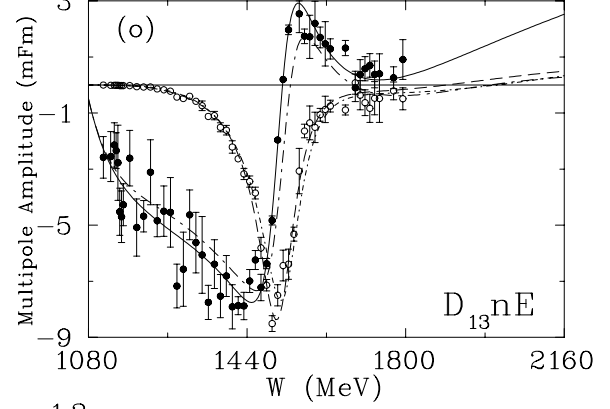
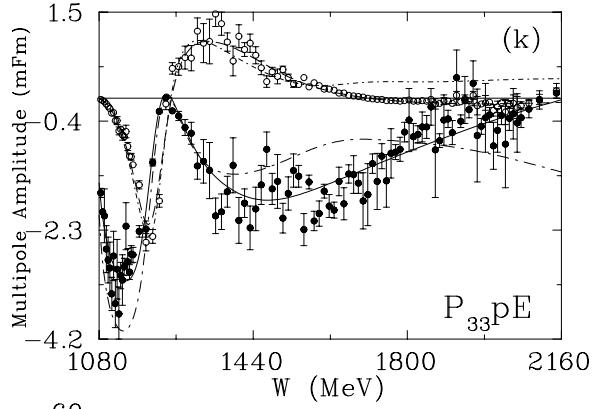
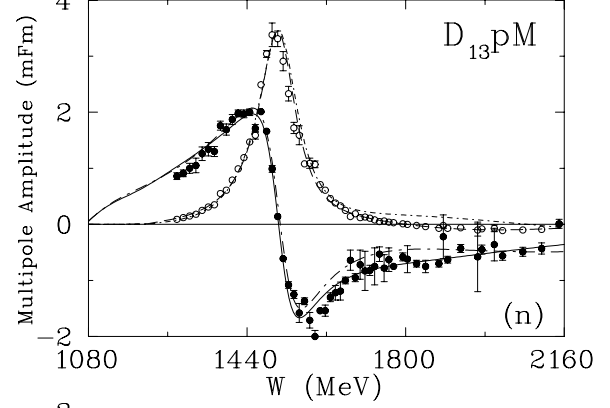
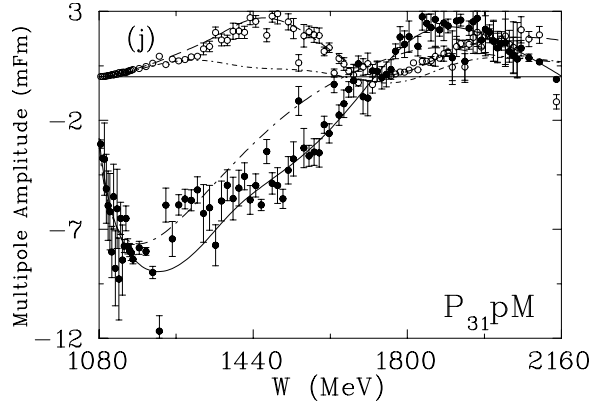
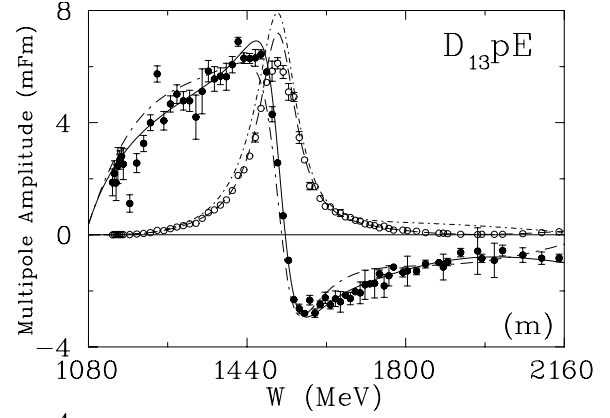
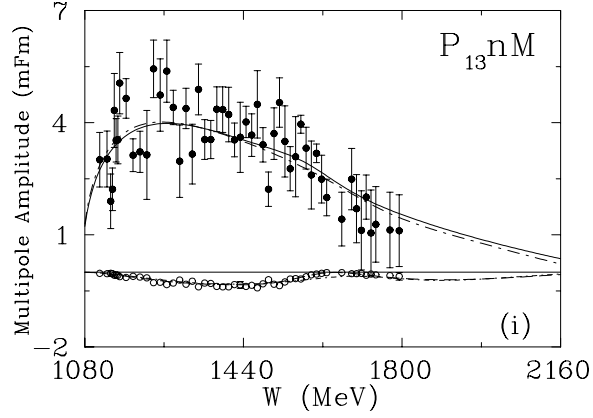


FIG. 1. Energy-angle distribution of recent (post-1995) data: (a) unpolarized $\pi^0 p$, (b) polarized $\pi^0 p$, (c) unpolarized $\pi^+ n$, (d) polarized $\pi^+ n$. (a,c) total cross sections and (b,d) $(\sigma_{1/2} - \sigma_{3/2})$ are plotted at zero degrees.





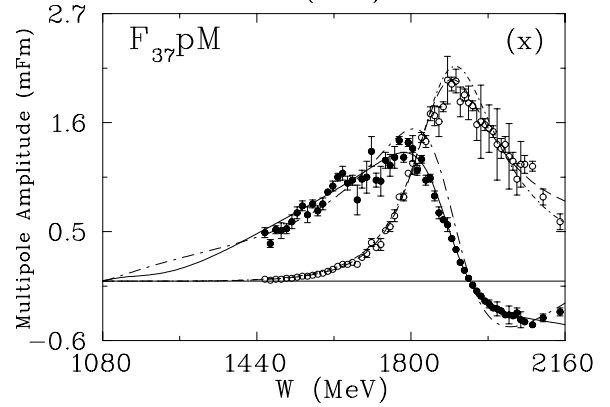
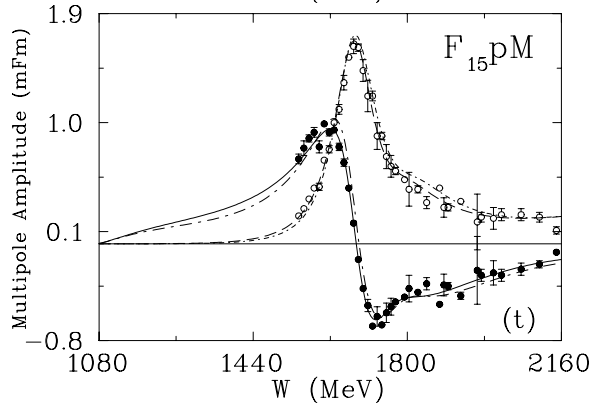
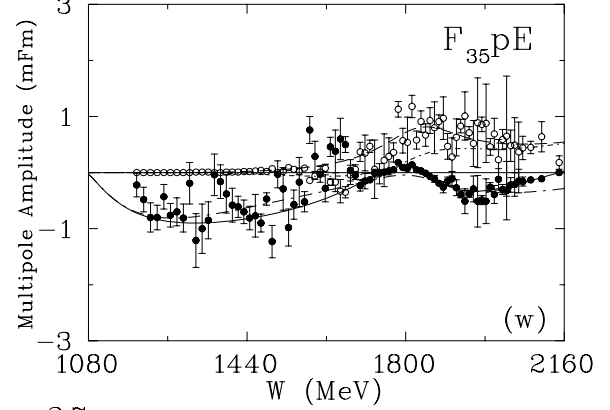
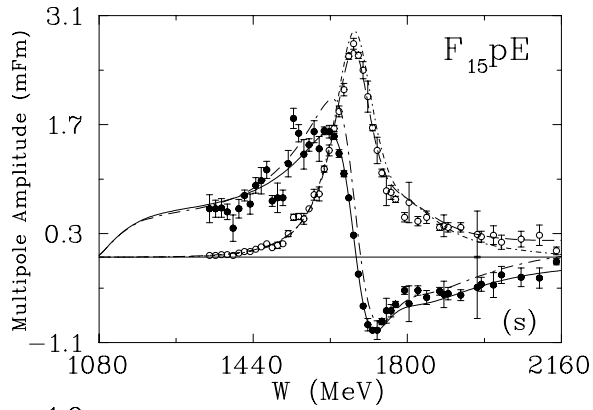
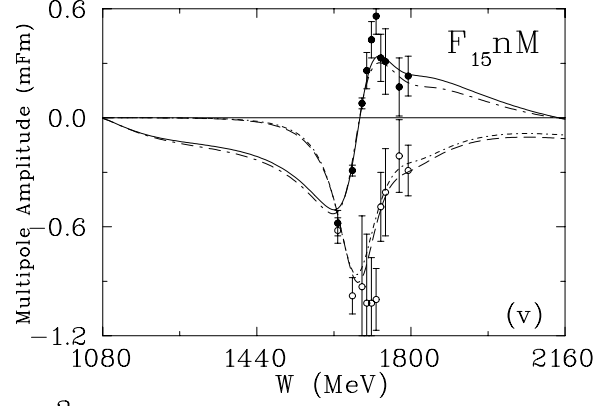
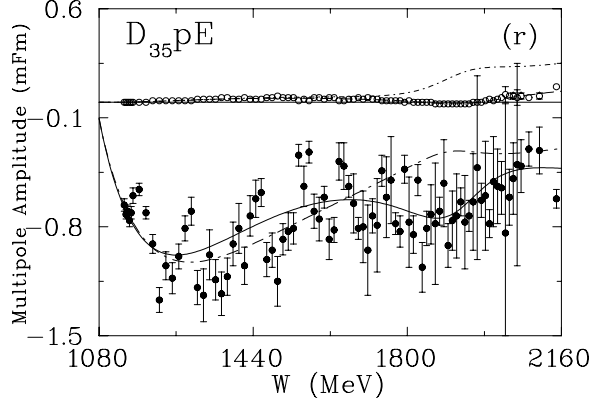
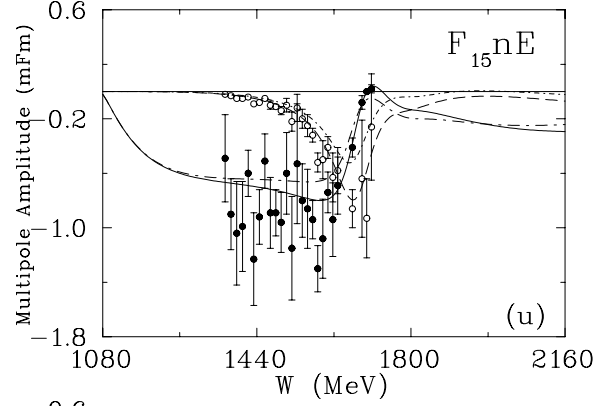
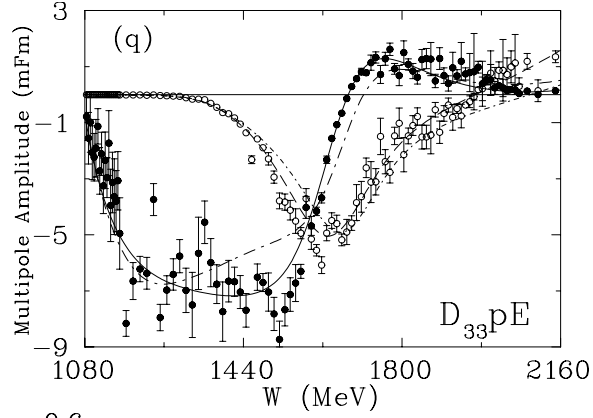


FIG. 2. Partial-wave amplitudes ($L_{2I,2J}$) from threshold to $E_\gamma = 2$ GeV. Solid (dashed) curves give the real (imaginary) parts of amplitudes corresponding to the SM02 solution. The real (imaginary) parts of single-energy solutions are plotted as filled (open) circles. The previous SM95 solution [5] is plotted with long dash-dotted (real part) and short dash-dotted (imaginary part) lines. Plotted are the multipole amplitudes (a) ${}_pE_{0+}^{1/2}$, (b) ${}_nE_{0+}^{1/2}$, (c) ${}_pE_{0+}^{3/2}$, (d) ${}_pM_{1-}^{1/2}$, (e) ${}_nM_{1-}^{1/2}$, (f) ${}_pE_{1+}^{1/2}$, (g) ${}_pM_{1+}^{1/2}$, (h) ${}_nE_{1+}^{1/2}$, (i) ${}_nM_{1+}^{1/2}$, (j) ${}_pM_{1-}^{3/2}$, (k) ${}_pE_{1+}^{3/2}$, (l) ${}_pM_{1+}^{3/2}$, (m) ${}_pE_{2-}^{1/2}$, (n) ${}_pM_{2-}^{1/2}$, (o) ${}_nE_{2-}^{1/2}$, (p) ${}_nM_{2-}^{1/2}$, (q) ${}_pE_{2-}^{3/2}$, (r) ${}_pE_{2+}^{3/2}$, (s) ${}_pE_{3-}^{1/2}$, (t) ${}_pM_{3-}^{1/2}$, (u) ${}_nE_{3-}^{1/2}$, (v) ${}_nM_{3-}^{1/2}$, (w) ${}_pE_{3-}^{3/2}$, and (x) ${}_pM_{3+}^{3/2}$. The subscript p (n) denotes a proton (neutron) target.

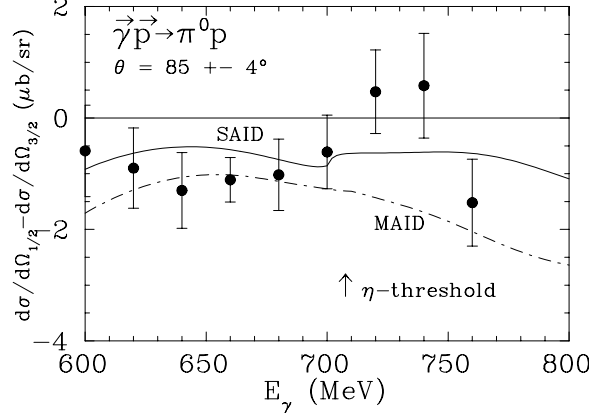


FIG. 3. Differential cross section ($d\sigma/d\Omega_{1/2} - d\sigma/d\Omega_{3/2}$) for $\vec{\gamma}\vec{p} \rightarrow \pi^0 p$ at $\theta = 85 \pm 4^\circ$. The solid (dash-dotted) line plots the SM02 (MAID2001 [44]) solution. Experimental data are from Mainz [45].

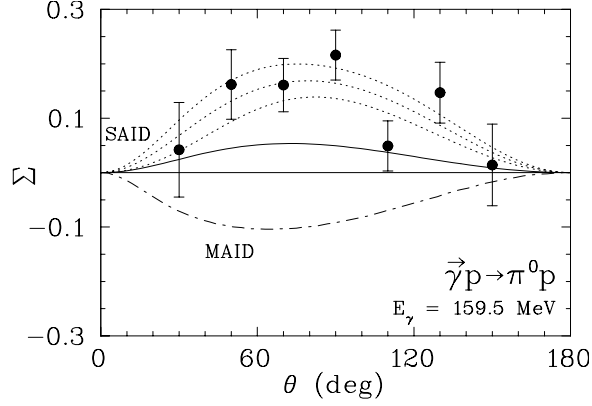


FIG. 4. Photon asymmetry for π^0 photoproduction on the proton at 159.5 MeV. Data are from Mainz (solid circles) [19]. Plotted are the SM02 (solid line), the 162 MeV-SES (158 – 165 MeV) fit associated with SM02 (dotted lines represent uncertainties of the SES fit) and the MAID2000 results (dash-dotted) [44].

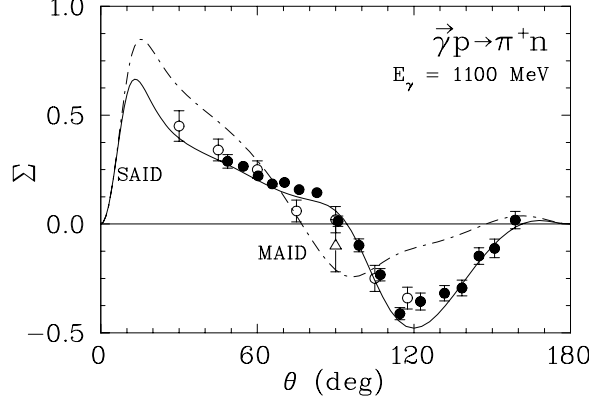


FIG. 5. Σ beam asymmetry for π^+n at 1100 MeV. Black circles show GRAAL results [25], open circles indicate the results of the Daresbury group [49], open triangles indicate the results from Saclay [50]. The solid (dash-dotted) line represents the SM02 (MAID2001 [44]) solution.

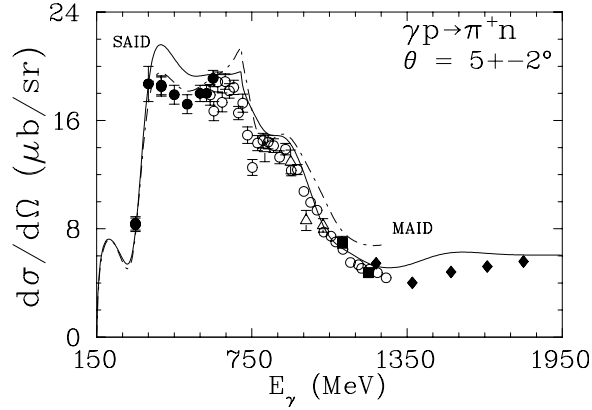


FIG. 6. Forward (5°) differential cross section for $\gamma p \rightarrow \pi^+n$ as a function of energy. Experimental data for the range of $5 \pm 2^\circ$ are from Orsay [51] (black circles), SLAC [52] (open circles), [53] (open triangles), [54] (black square), and DESY [55] (black diamonds.) The solid (dash-dotted) line represents the SM02 (MAID2001 [44]) solution.

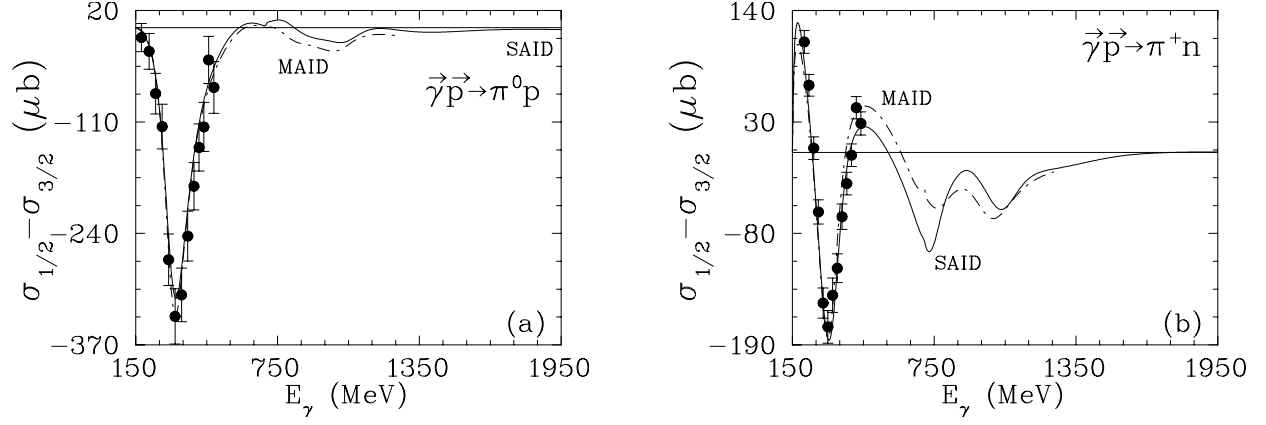


FIG. 7. Difference of the total cross sections for the helicity states 1/2 and 3/2. (a) $\vec{\gamma}\vec{p} \rightarrow \pi^0 p$ and (b) $\vec{\gamma}\vec{p} \rightarrow \pi^+ n$. The solid (dash-dotted) line represents the SM02 (MAID2001 [44]) solution. Experimental data are from Mainz [15].

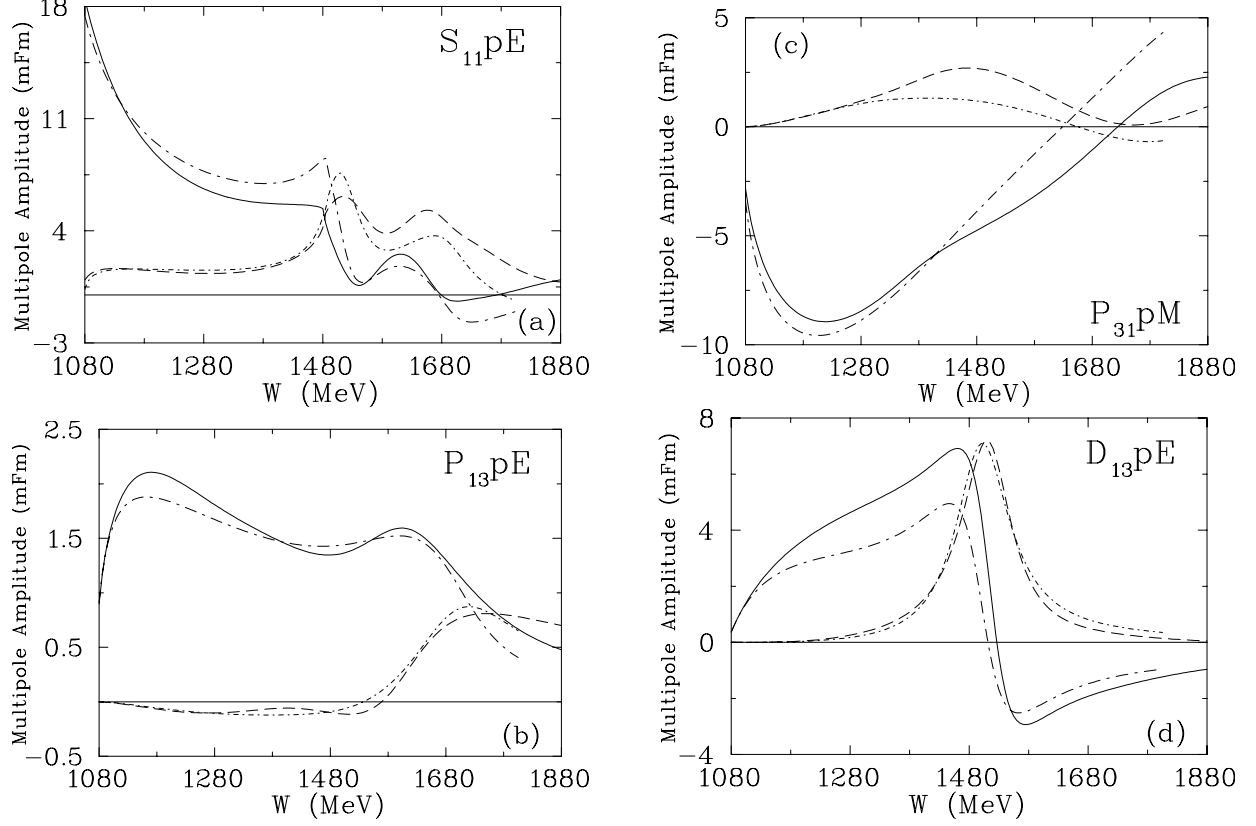


FIG. 8. Selected partial-wave amplitudes to $E_\gamma = 1250$ MeV. Solid (dashed) curves give the real (imaginary) parts of amplitudes corresponding to the SM02 solution. The recent MAID2001 solution [44] is plotted with long dash-dotted (real part) and short dash-dotted (imaginary part) lines. Plotted are the multipole amplitudes (a) $S_{11}pE$ [${}_pE_{0+}^{1/2}$], (b) $P_{13}pE$ [${}_pE_{1+}^{1/2}$], (c) $P_{31}pM$ [${}_pM_{1-}^{3/2}$], and (d) $D_{13}pE$ [${}_pE_{2-}^{1/2}$]. The subscript p (n) denotes a proton (neutron) target.

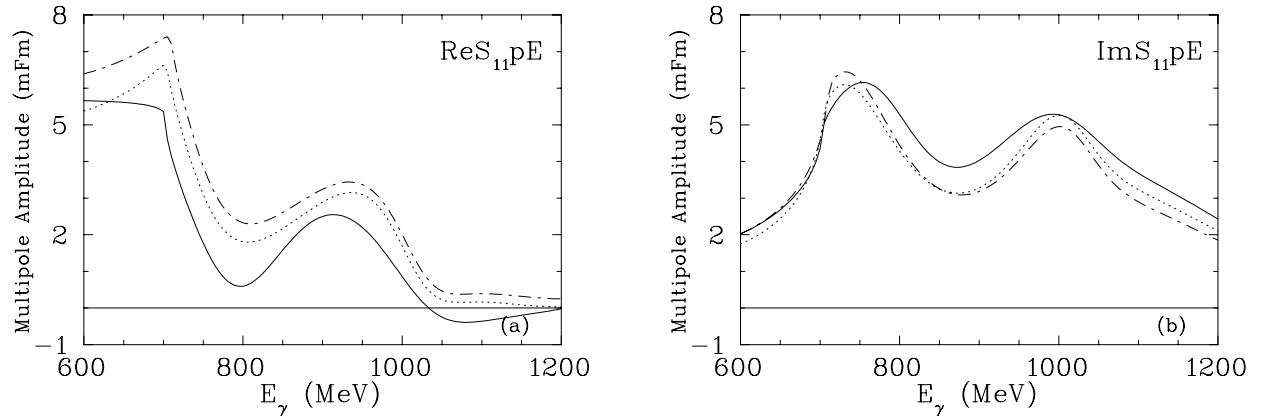


FIG. 9. $S_{11}pE$ multipole for 600 to 1200 MeV. Plotted are (a) real part and (b) imaginary part. The SM02 (SX99) solution is plotted with a solid (dashed) line and previous SM95 solution [5] with a dash-dotted line.

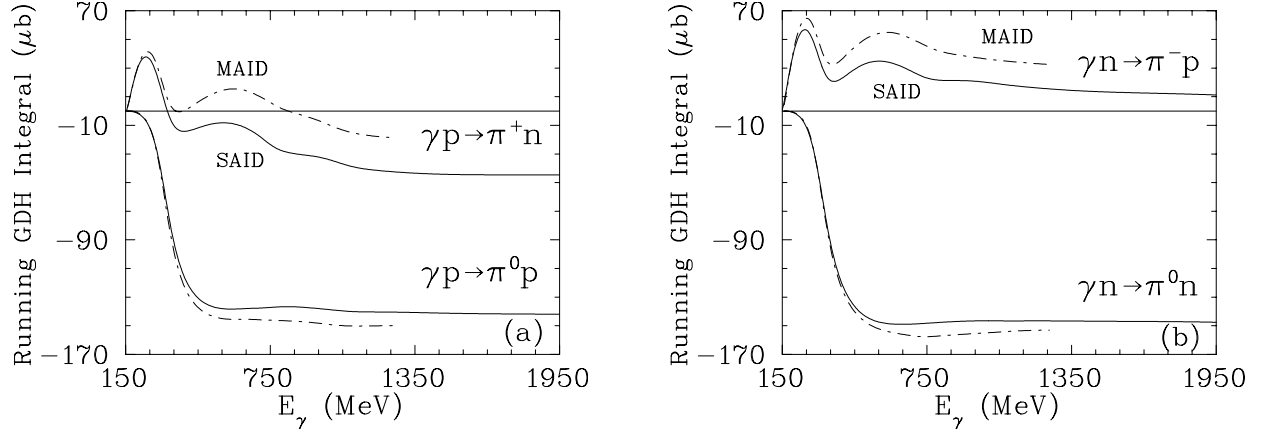


FIG. 10. Running GDH integral. (a) for proton and (b) neutron targets. The solid (dash-dotted) line represents the SM02 (MAID2000 [44]) solution.

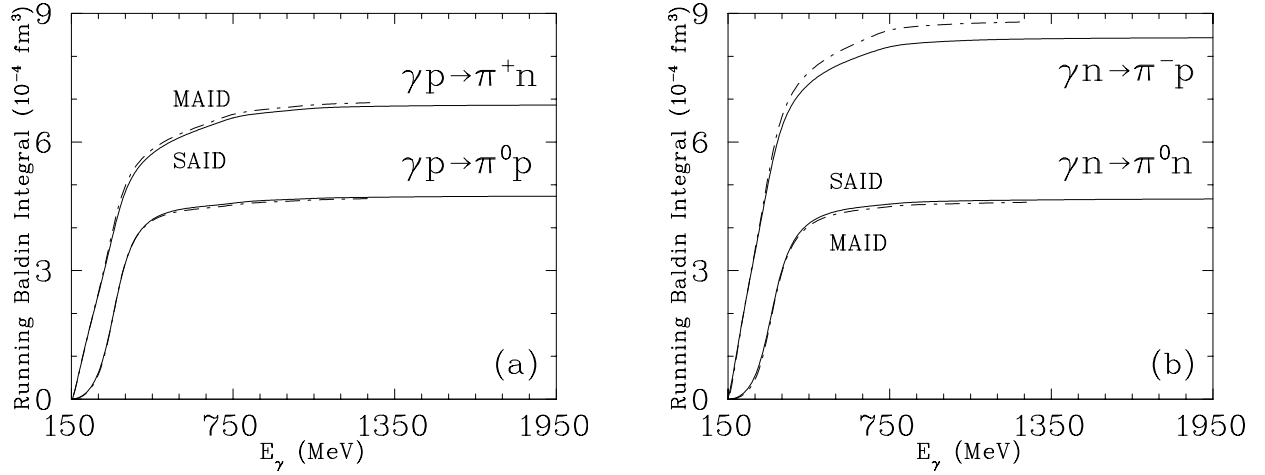


FIG. 11. Running Baldin integral. (a) for proton and (b) neutron targets. The solid (dash-dotted) line represents the SM02 (MAID2000 [44]) solution.

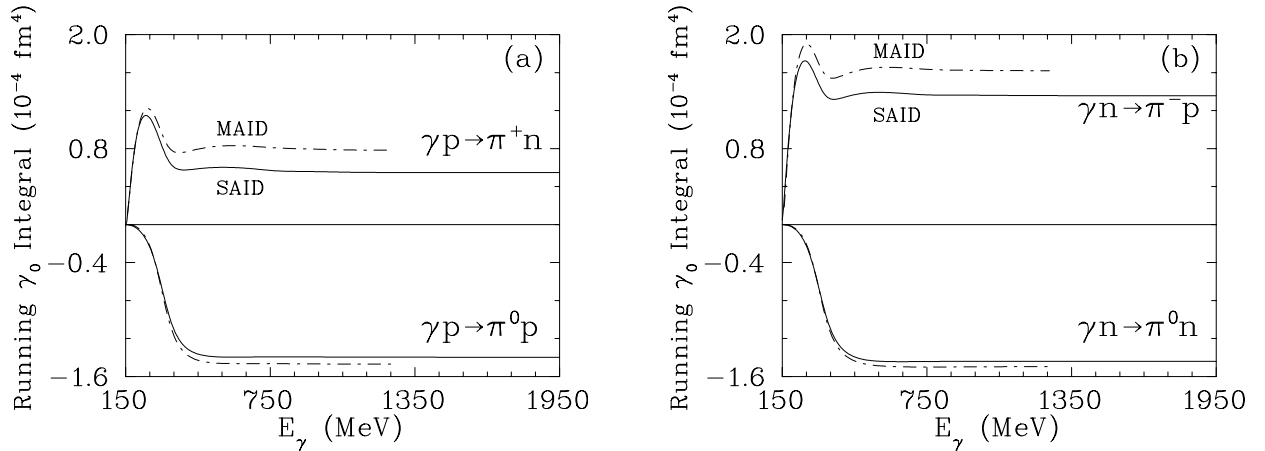


FIG. 12. Forward spin polarizability γ_0 . (a) for proton and (b) neutron targets. The solid (dash-dotted) line represents the SM02 (MAID2000 [44]) solution.